Remote sensing of mixing-layer height at ICOS and TERENO stations

Stefan Emeis
Institute for Meteorology and Climate Research
Atmospheric Environmental Research Division (IMK-IFU)
Karlsruhe Institute of Technology (KIT)
Kreuzeckbahnstr. 19
82467 Garmisch-Partenkirchen, Germany
E-mail: stefan.emeis@kit.edu

IMK-IFU

and its activities in TERENO

Dezember 2009

Betriebs- und Sicherheitsbeauftragte:

Sifa	E. Langer
Sibe	St. Schmid
SSB	Prof. Dr. H. Papen
Laser	Dr. T. Trickl
S1	Dr. S. Louis

Institut für Meteorologie und Klimaforschung (IMK-IFU)

Bereich Atmosphärische Umweltforschung

Leiter: Prof. Dr. Hans Peter Schmid
Stellvertreter: Prof. Dr. Hans Papen

Kst. 5260

Informationstechnologie und Organisation
Leiter: Dipl.Ing. Heiner Stengel
Stellvertreter: Reiner Müller

Assistenz
Monika Liebl-Rombach

Austauschprozesse in komplexem Terrain
Prof. Dr. Hans Peter Schmid

Ecological Observatorium TERENO-alpine
Prof. Dr. Hans Papen

World Calibration Center (WCC)
Dr. Hans-Eckhart Scheel

Bio-Geo-Chemische Prozesse

Leiter: Prof. Dr. Klaus Butterbach-Bahl
Stellvertreter: Prof. Dr. Hans Papen; Prof. Dr. Jörg-Peter Schnitzler

- **Ökosystemare Stoffströme**
  Prof. Dr. Hans Papen
- **Biologische Prozesse**
  Prof. Dr. Jörg-Peter Schnitzler
- **Zentrum für stabile Isotope (CSI)**
  Dr. Nicolas Brüggemann
- **Regionalisierung von Spurengasemissionen**
  Prof. Dr. Klaus Butterbach-Bahl

Regionale Klimasysteme

Leiter: Prof. Dr. Harald Kunstmann
Stellvertreter: Dr. Ralf Sussmann

- **Atmosphärische Variabilität und Trends**
  Dr. Ralf Sussmann
- **Luftqualität in Ballungsräumen und sensitiven Regionen**
  Dr. Peter Suppan
- **Gekoppelte numerische Modellsysteme**
  Dr. Rüdiger Grote
- **Klimaänderung und terrestrischer Wasserhaushalt**
  Prof. Dr. Harald Kunstmann

personnel

58 employees
- 35 scientists
- 12 engineers and technicians
- 11 staff

21 PhD/Diploma students (Italy, China, Australia, etc.)

5 postdoc / guests

7 interns, etc.

---

91 persons in total

IMK-IFU „Highlights“

New greenhouse (06.10.2009)

TERENO

TERRESTRIAL ENVIRONMENTAL OBSERVATORIES

The Bavarian Prealpine Observatory

Hans Peter Schmid, Harald Kunstmann, Hans Papen, Jean Charles Munch, Eckart Priesack

HELMHOLTZ ASSOCIATION

The Bavarian Prealpine Observatory

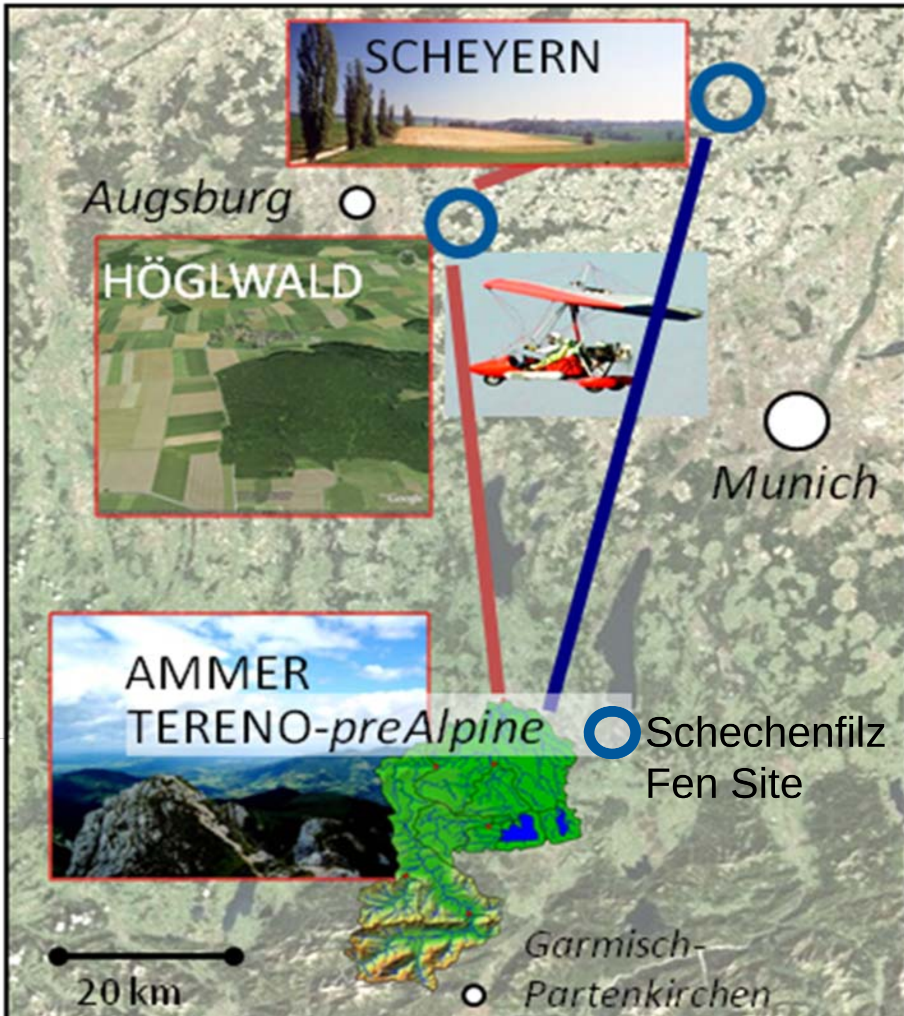

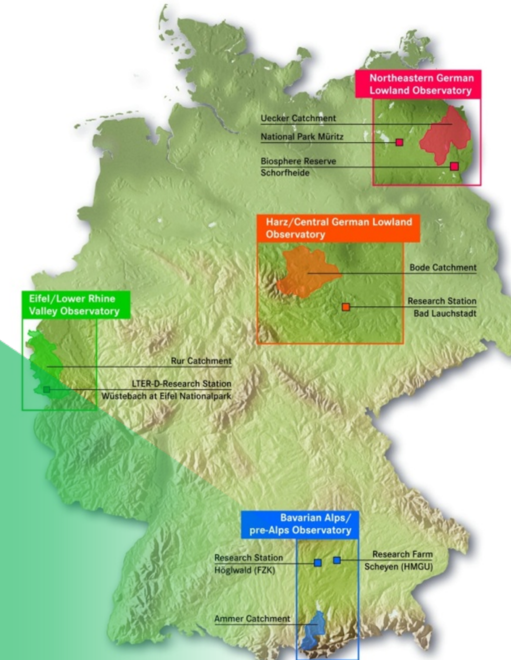

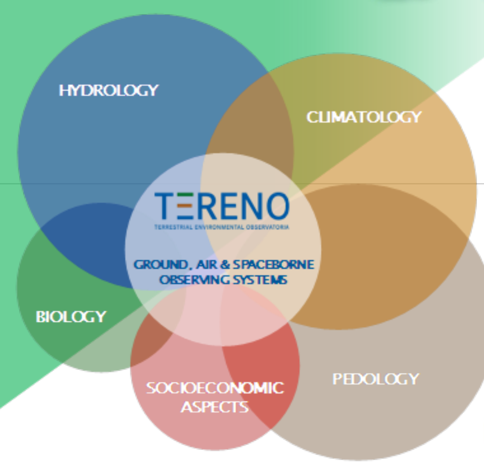

HELMHOLTZ | ASSOCIATION

"In House" Research Goals

- Long-Term **biosphere-atmosphere exchange** (greenhouse gases, energy balance)
- Coupled **C-/N-cycles** and C-/N-storage
- **Vegetation and microbial biodiversity** (temporal dynamics, relation to matter turnover)
- **Alpine watershed hydrology** (water budget, Karst related problems, precipitation variability, floods/droughts, seepage water quality/quantity, water retention capacity)
- **Nutrient deposition** and **land use/management** (wet grasslands/fens, forests and agricultural systems).
- **Methodology development** for micrometeorological observations in complex terrain

Ammer Catchment Observatory

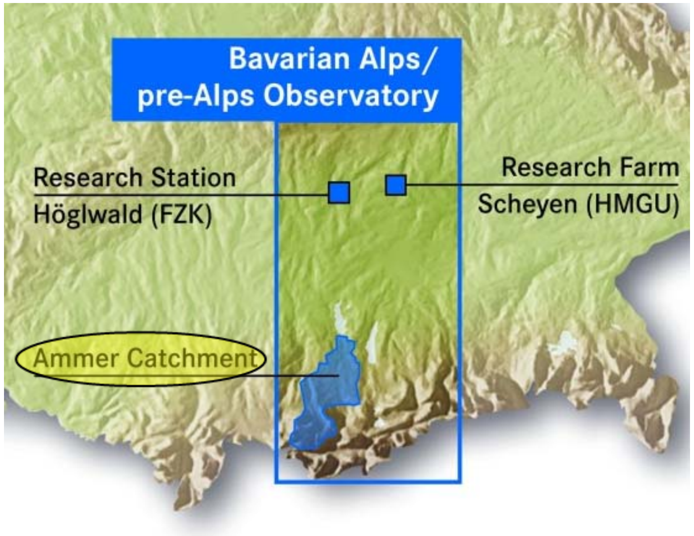

- area of ~710 km² (601 km² above Weilheim)
- alpine and prealpine landscape with high spatial differentiation in geology and pedology
- elevations: from 533 m (a.s.l., Ammersee) to 2185 m (Kreuzspitze)
- two dominant landscape units: the prealpine hill country and moorland and the Swabian-Upper Bavarian foothills of the Alps.
- Dominant geology: lime-alpine zone (south), flysch zone (north)

TERENO Infrastructure

- **Graswang-, Rottenbuch-, Fendt Sites**
  - 3 EC towers: momentum, heat, H_2O, CO_2, plus TERENO-ICOS: N_2O, CH_4 fluxes
  - 36 Lysimeters: soil water balance,
  - GHG (N_2O, CO_2, CH_4) measurements at lysimeters
- **Geigersau Site:** 1 X-Band precipitation radar
- **Sites to be determined:** 3 Climate stations

prealpine TERENO TERRESTRIAL ENVIRONMENTAL OBSERVATORIES

Climasequence: how do grassland ecosystems adapt to climate change?

- grassland soil monoliths transplanted along the natural gradient in temperature and precipitation
- climate change effects on C/N cycles
- associated plant and microbial processes/populations/biodiversity
- terrestrial hydrology and water quality

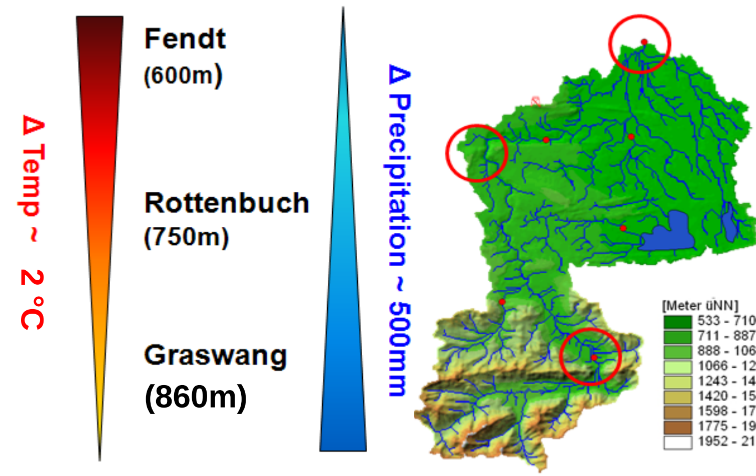

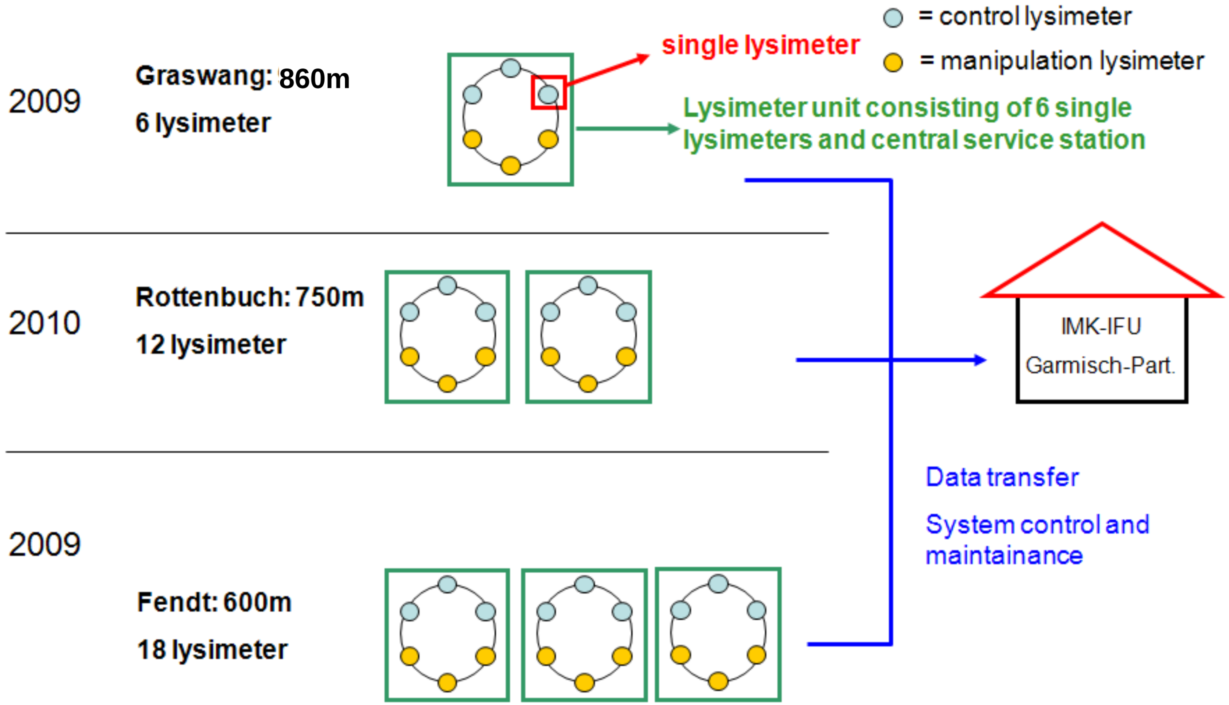

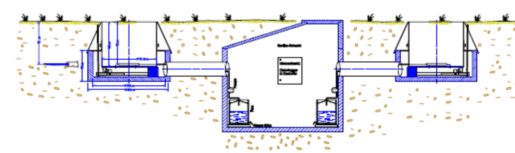

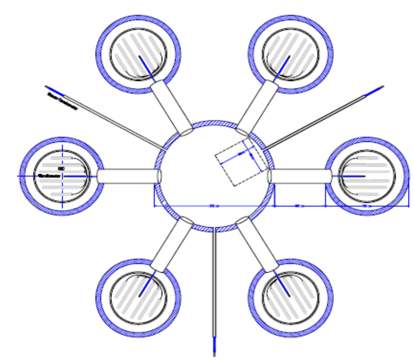

HELMHOLTZ | ASSOCIATION

TERENO Lysimeter experiment: construction phase

TERENO rain RADAR Geigersau

HELMHOLTZ ASSOCIATION

prealpine

TERENO
TERRESTRIAL ENVIRONMENTAL OBSERVATORIES

Observations and Meso-Scale Modelling of Alpine Watershed Hydrology

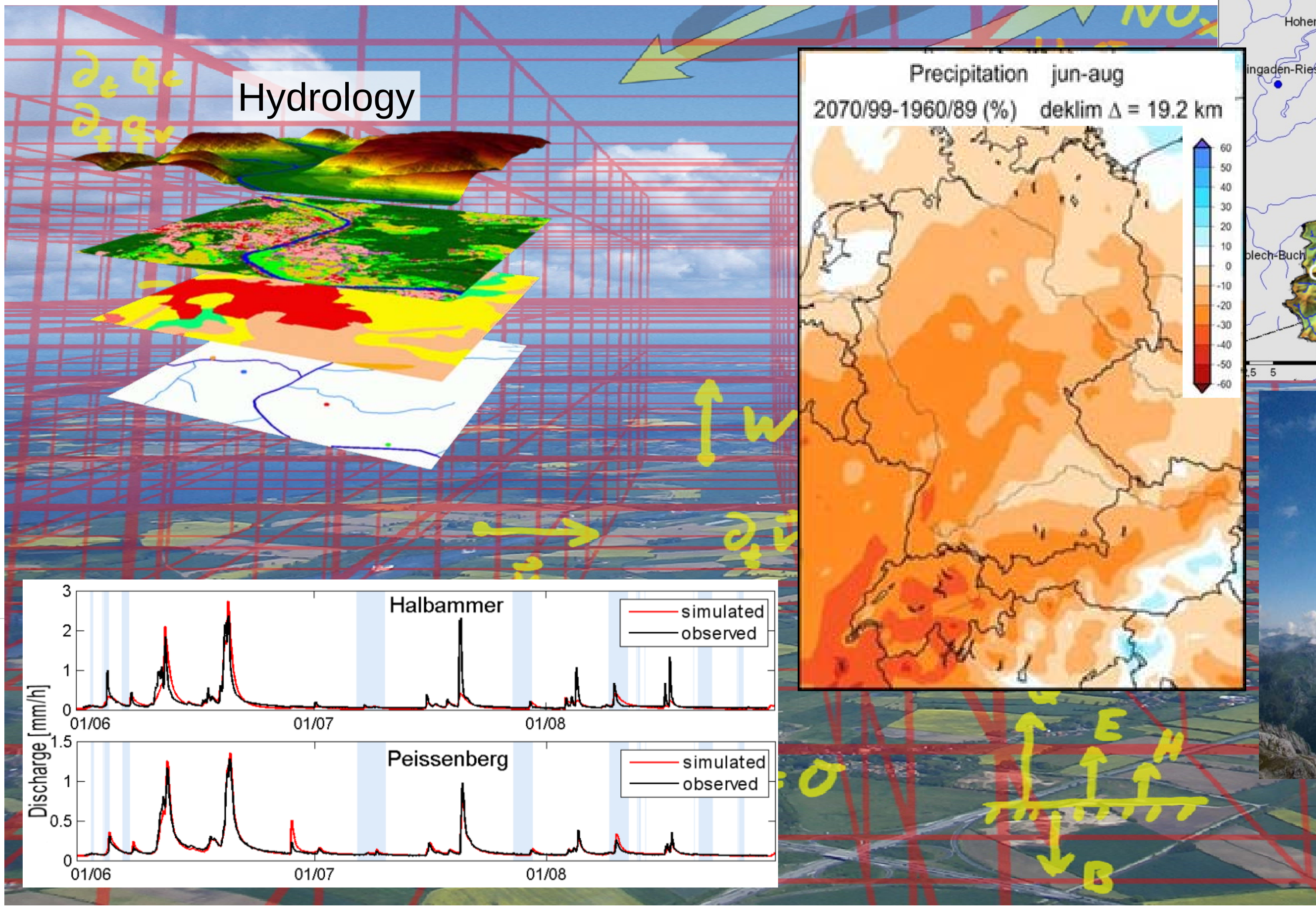

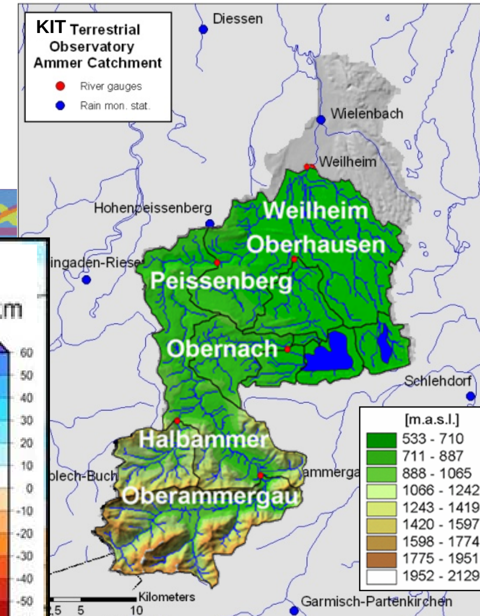

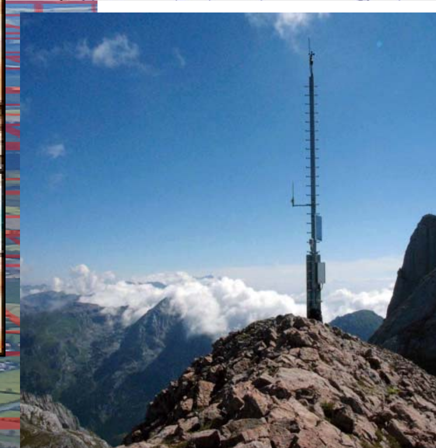

HELMHOLTZ | ASSOCIATION

TERENO
TERRESTRIAL ENVIRONMENTAL OBSERVATORIES

icos integrated carbon observation system

A European infrastructure dedicated to high precision monitoring of greenhouse gas fluxes

http://www.icos-infrastructure.eu/

- ICOS mission: “To provide the long-term observations required to understand the present state and predict future behavior of the global carbon cycle and greenhouse gas emissions.”
- 5 EC-sites at TERENO-prealpine, -Harz, and –Eifel received additional funding to expand instrumentation to include fluxes of CH_4 and N_2O and upgrade to ICOS standard

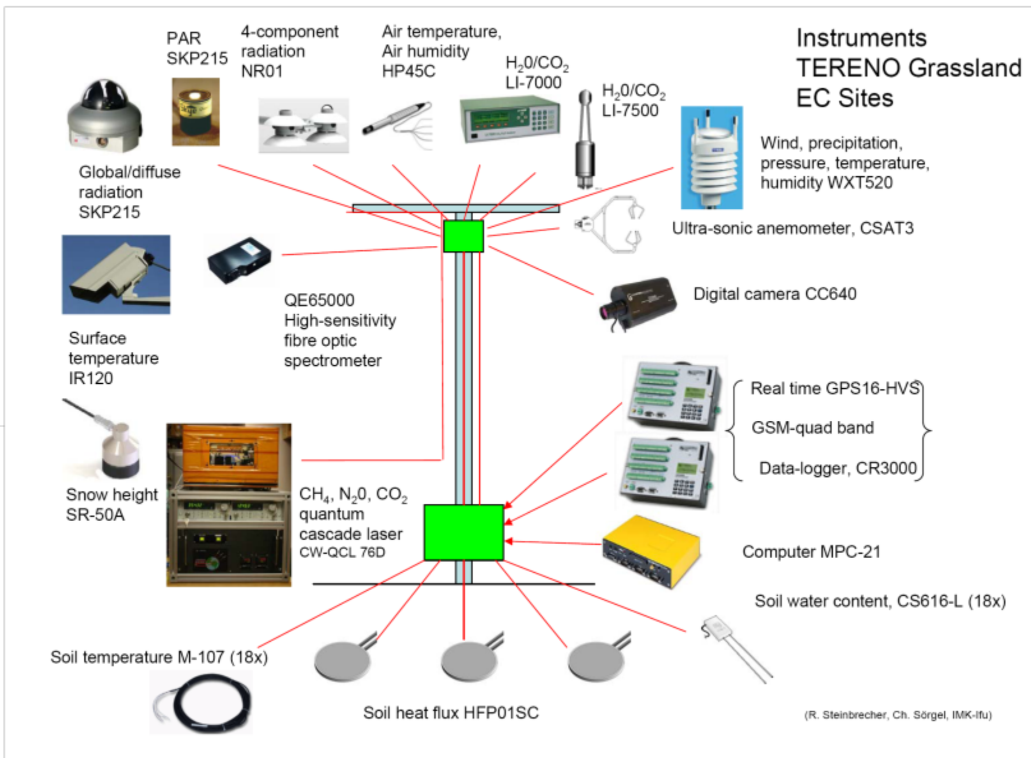

HELMHOLTZ | ASSOCIATION

Remote sensing

of the vertical structure of the atmospheric boundary layer

Motivation

correlation at street level pollutant - MLH

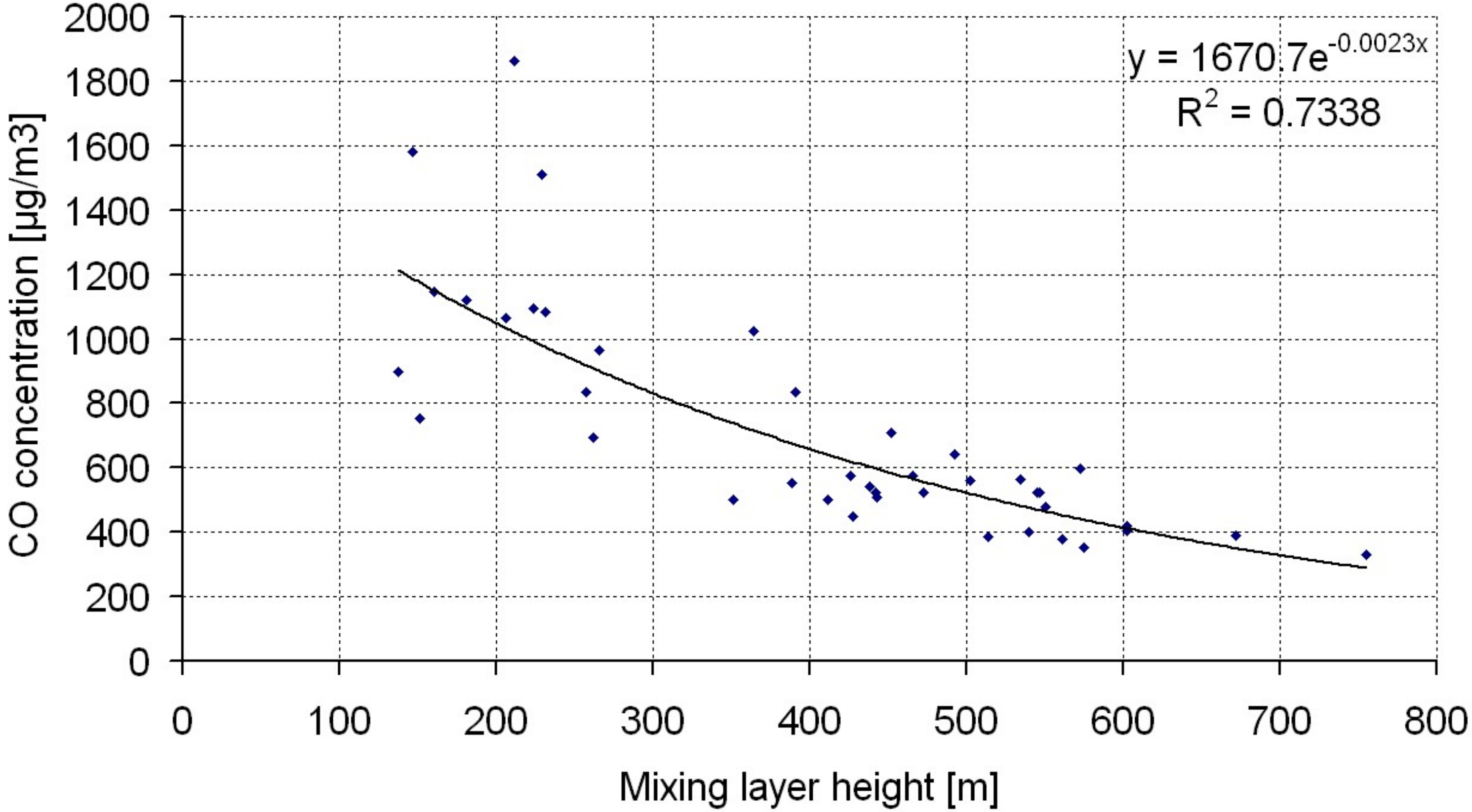

Schäfer, K., S. Emeis, H. Hoffmann, C. Jahn, 2006: Influence of mixing layer height upon air pollution in urban and sub-urban areas. Meteorol. Z., 15, 647-658.

Typical frequency bands for remote sensing of the atmosphere

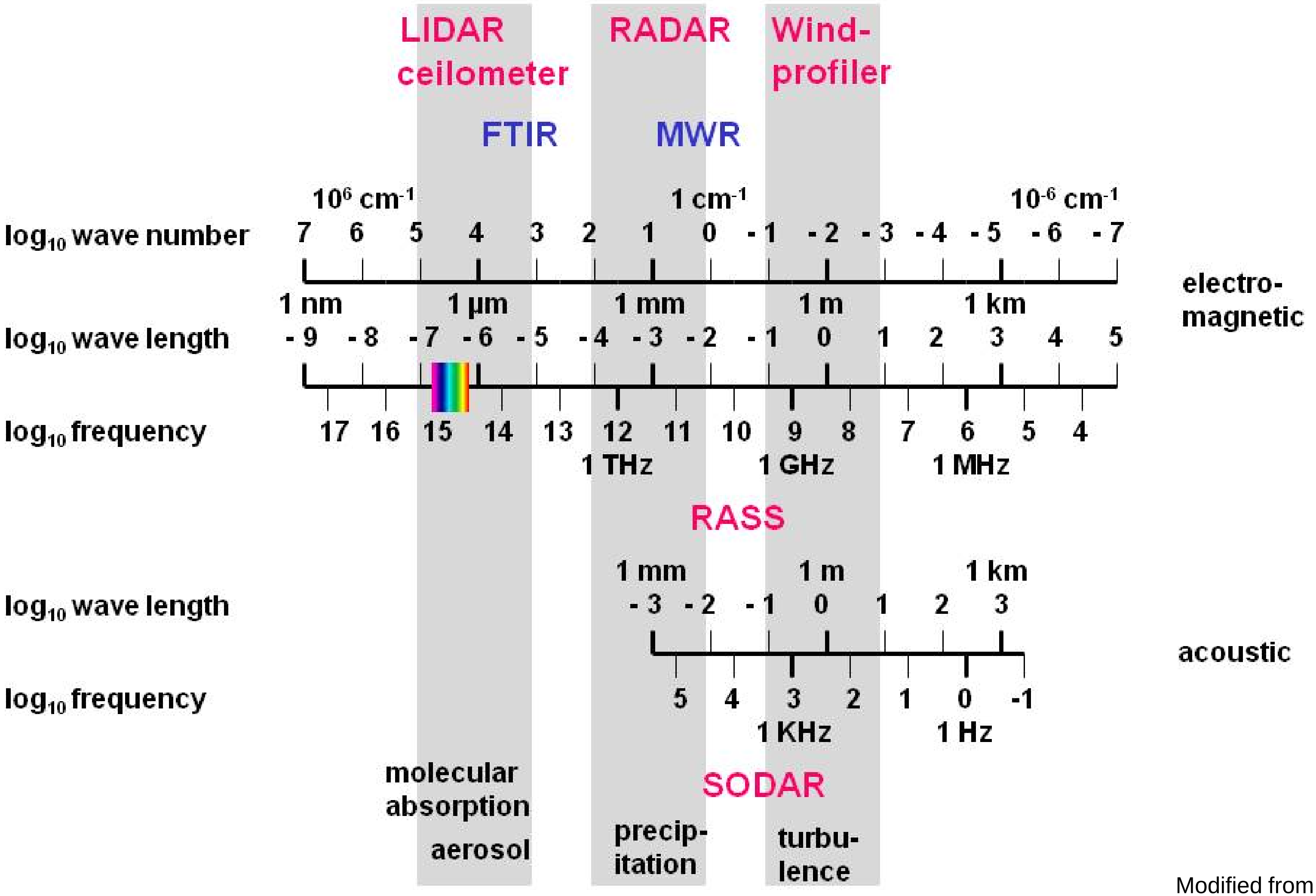

Modified from Fig. 8.1 in „Meteorologie in Stichworten“, Borntraeger, Berlin Stuttgart 2000

Basic remote sensing techniques

subject of this talk

name	princple	spatial resolution	direction	type
RADAR	backscatter, electro-magnetic pulses, fixed wave length	profiling	scanning, slanted	active, monostatic
SODAR	backscatter, acoustic pulses, fixed wave length	profiling	fixed, slanted, vertical	active, usually monostatic
LIDAR	backscatter, optical pulses, fixed wave length(s)	profiling	scanning, fixed, horizontal, slanted, vertical	active, monostatic
RASS	backscatter, acoustic, electro-magnetic, fixed wave length	profiling	fixed, vertical	active, monostatic
	absorption, infrared, spectrum	path-averaging	fixed, horizontal, slanted	active, bistatic or passive
FTIR	emission, infrared, spectrum	path-averaging	fixed, horizontal, slanted	passive
DOAS	absorption, optical, fixed wave lengths	path-averaging	fixed, horizontal	active, bistatic
radiometry	electro-magnetic, fixed wave length(s)	averaging, profiling	fixed, scanning, slanted, vertical	passive
tomography	travel time, acoustic, fixed wave length	horizontal distribution	fixed, horizontal	active, multiple emitters and receivers

subject of this talk

SODAR

algorithms for mixing-layer height

monostatic SODAR: measuring principles

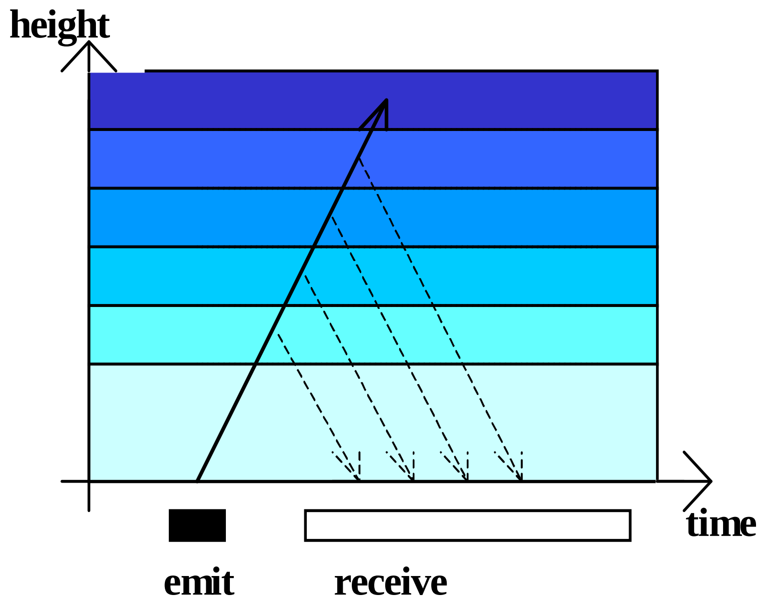

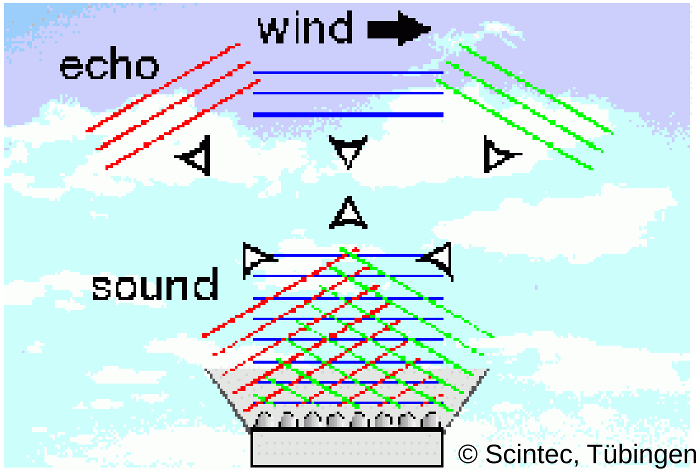

© Scintec, Tübingen

deduction:

sound travel time = height
backscatter intensity = turbulence
Doppler-shift = wind speed

Emission of sound waves into three directions:

in order to measure all three components of the wind (horizontal and vertical)

three-antenna SODAR
range: roughly 1 km

phased-array SODAR
range: roughly 600 m

Sample plot SODAR (convective BL at daytime)

acoustic backscatter intensity

sigma w

40 – 300 m

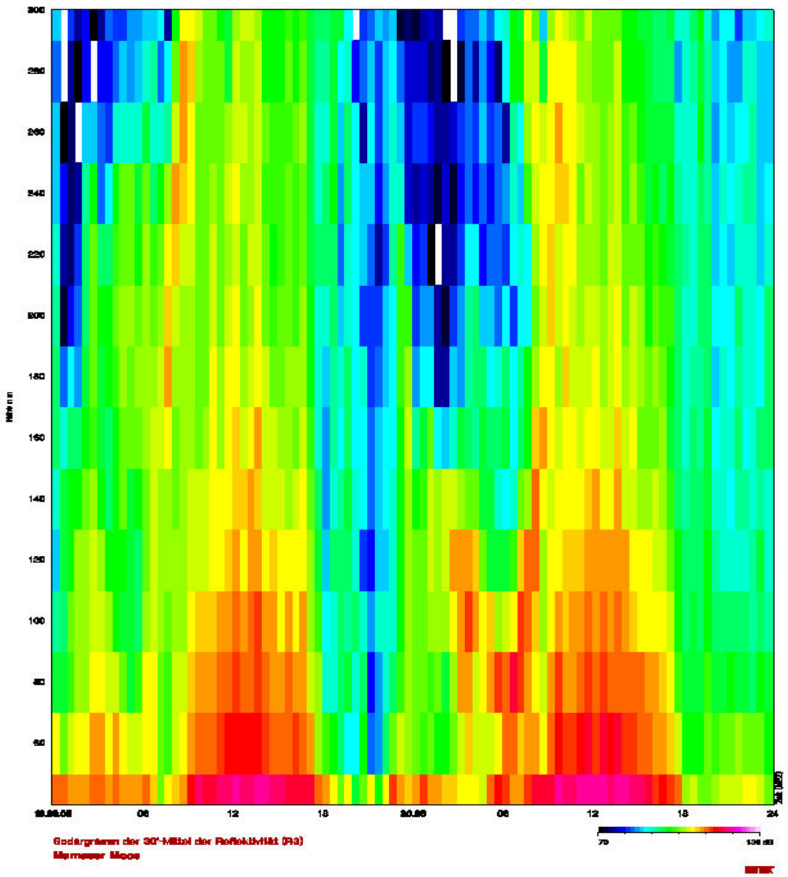

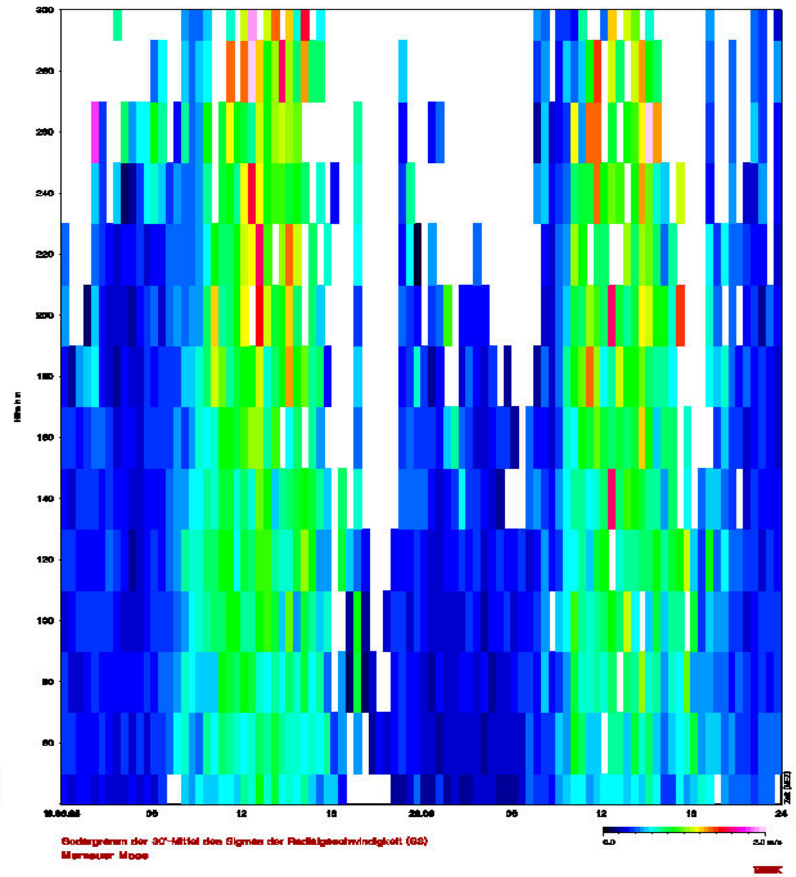

2 days, midnight to midnight

Sample plot SODAR (lifted inversion)

acoustic backscatter intensity

sigma w

40 – 400 m

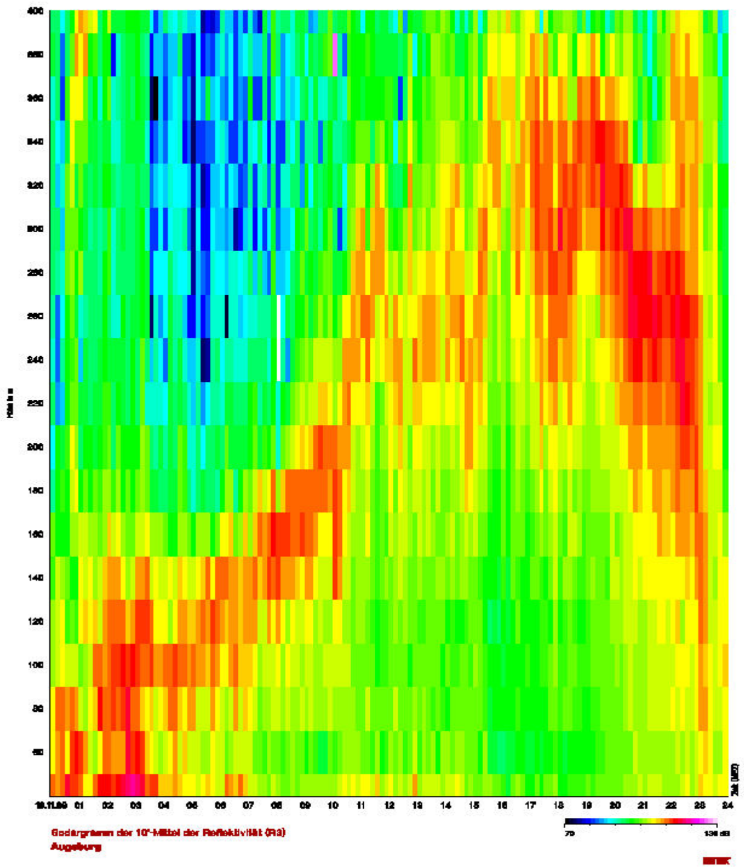

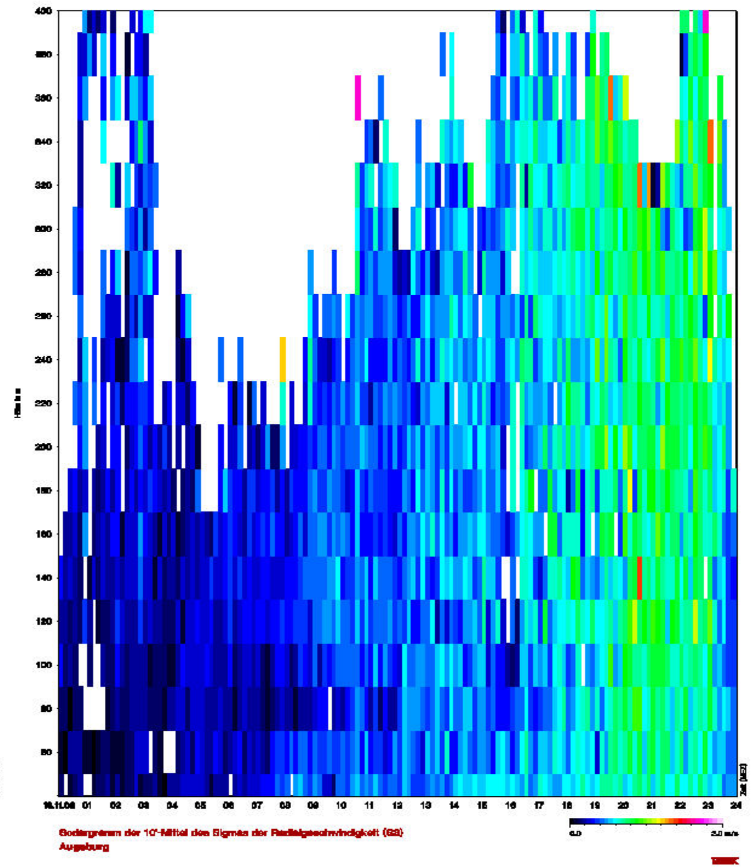

1 day, midnight to midnight

Algorithms to
detect MLH
from SODAR data

criterion 1:
upper edge
of high
turbulence

criterion 2:
surface and
lifted
inversions

MLH = Min (C1, C2)

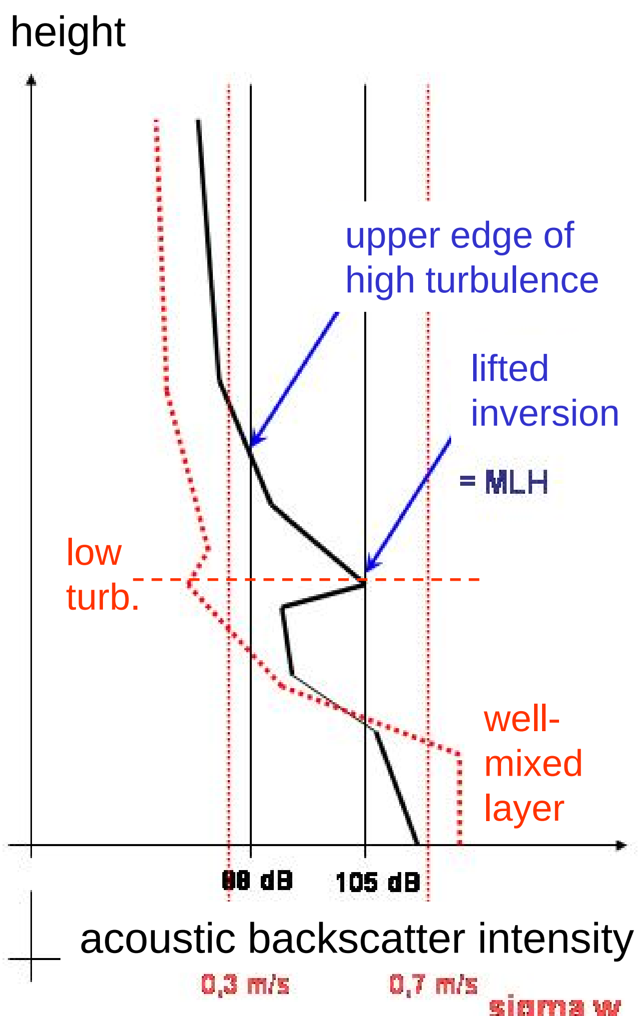

example 1: daytime

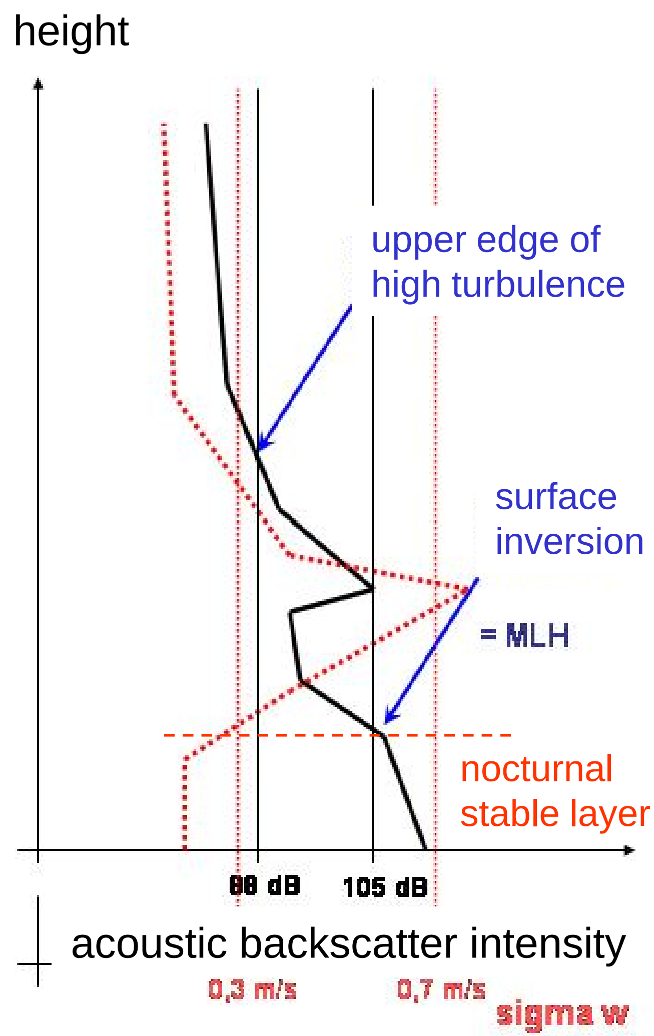

example 2: night-time

Ceilometer

algorithms for mixing-layer height

Ceilometer/LIDAR measuring principle

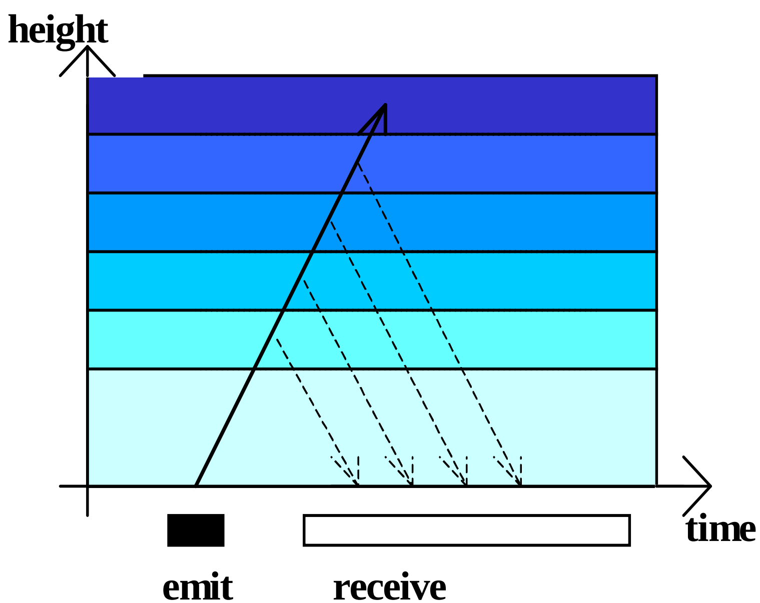

detection:

travel time of signal = height
backscatter intensity = particle size and number distribution
Doppler-shift = cannot be analyzed from ceilometer data
(only from Wind-LIDAR: velocity component in line of sight)

Sample plot ceilometer (convective BL at daytime)

optical backscatter intensity	negative vertical gradient of optical backscatter intensity

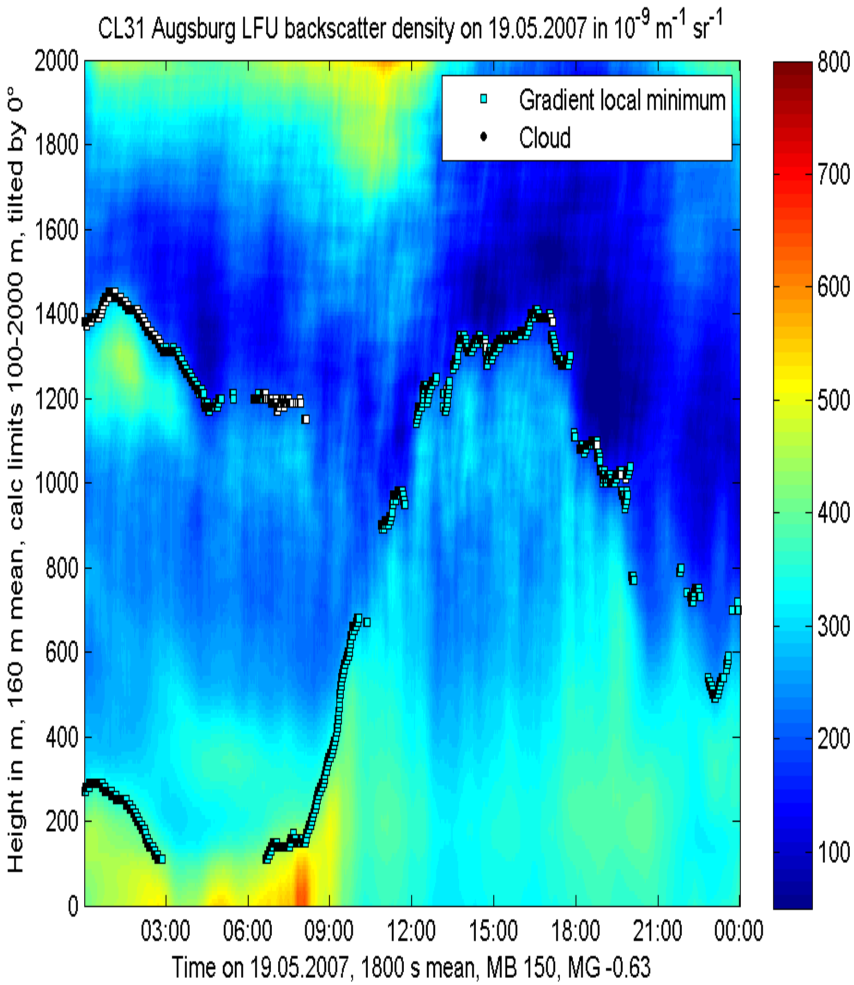

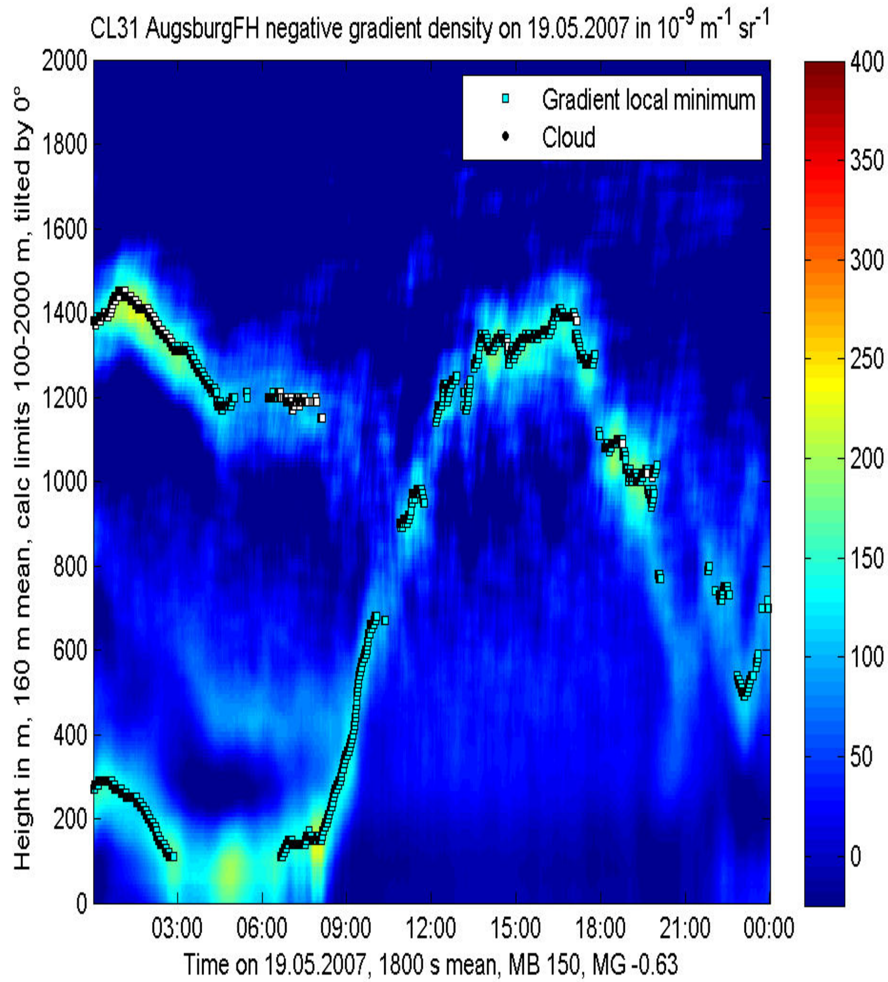

Algorithms to
detect MLH
from Ceilometer-Daten

criterion

minimal vertical gradient
of backscatter
intensity (the most
negative gradient)

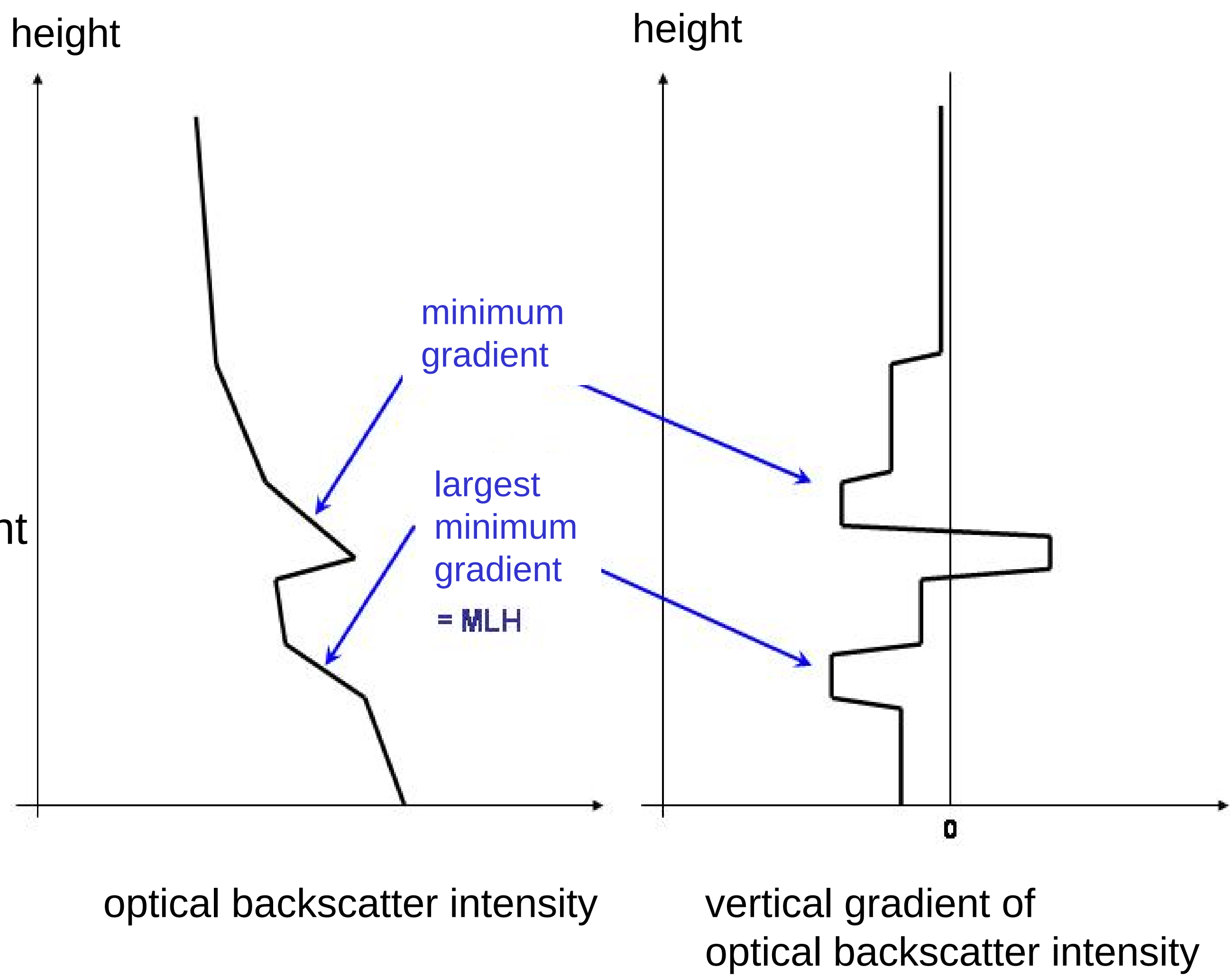

Different gradient methods (see Sicard et al. 2006, BLM 119, 135-157)

logarithmic gradient minimum

gradient minimum

inflection point method
(minimum of 2nd derivative)

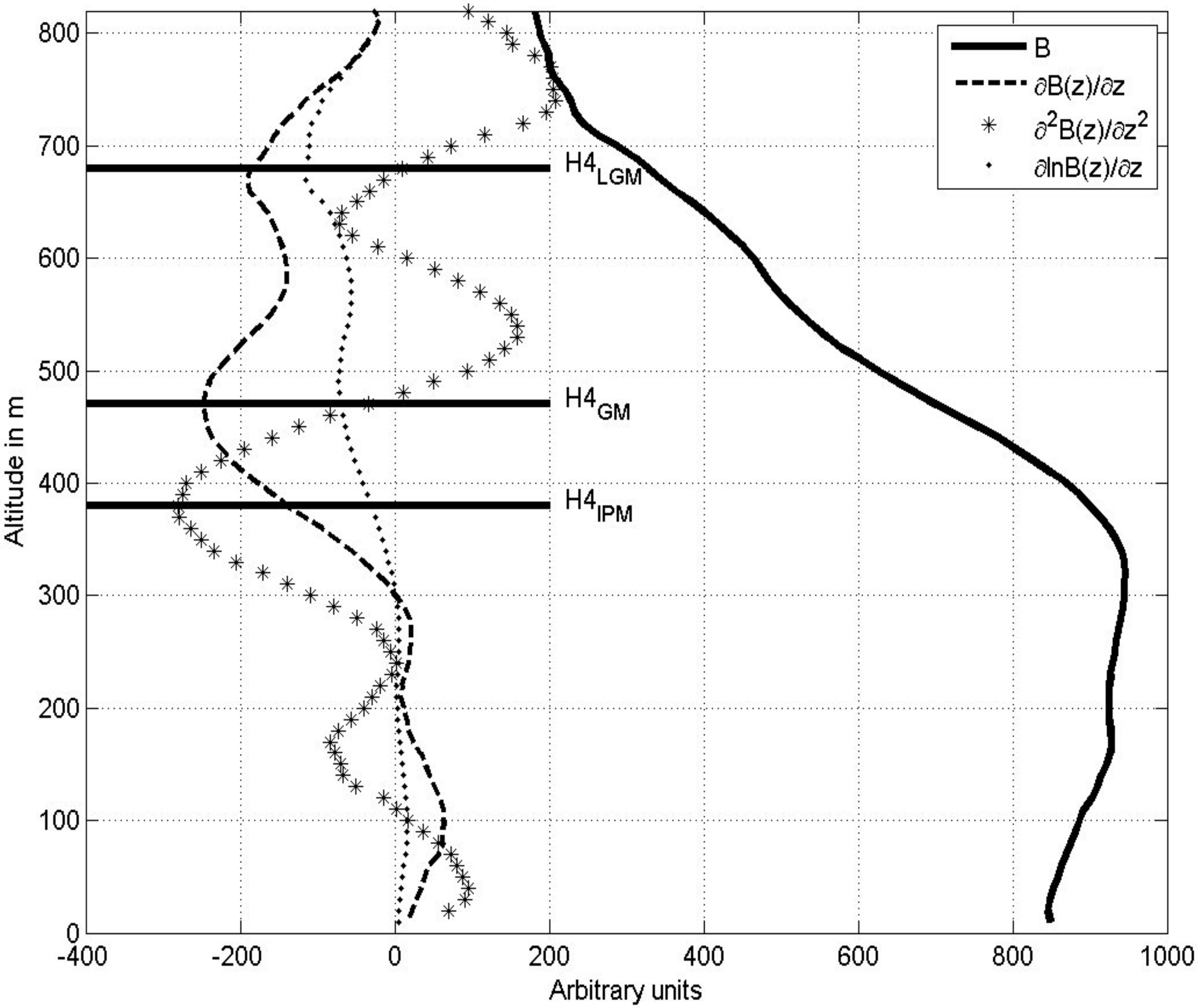

comparison of two different ceilometers

LD40

two optical axes
- wave length: 855 nm
- height resolution: 7.5 m
- max. range: 13000 m

CL31

one optical axis
- wave length: 905 nm
- height resolution: 5 m
- max. range: 7500 m

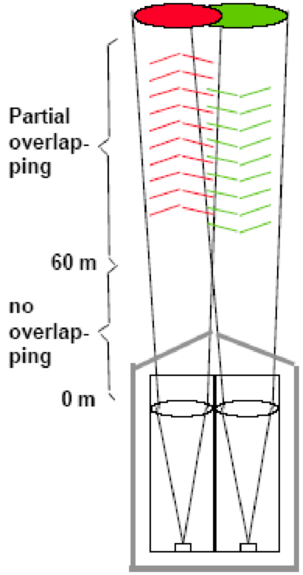

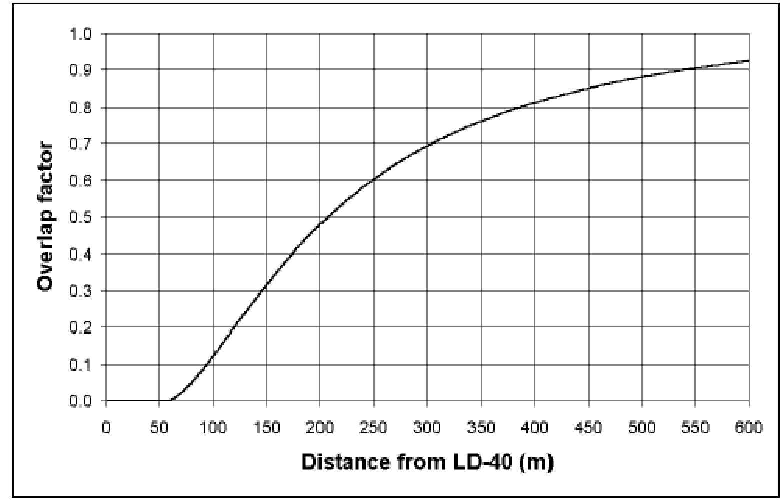

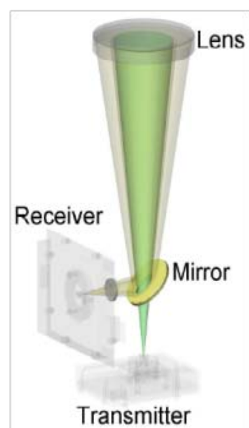

19 May 2007: ceilometer LD40 and CL31

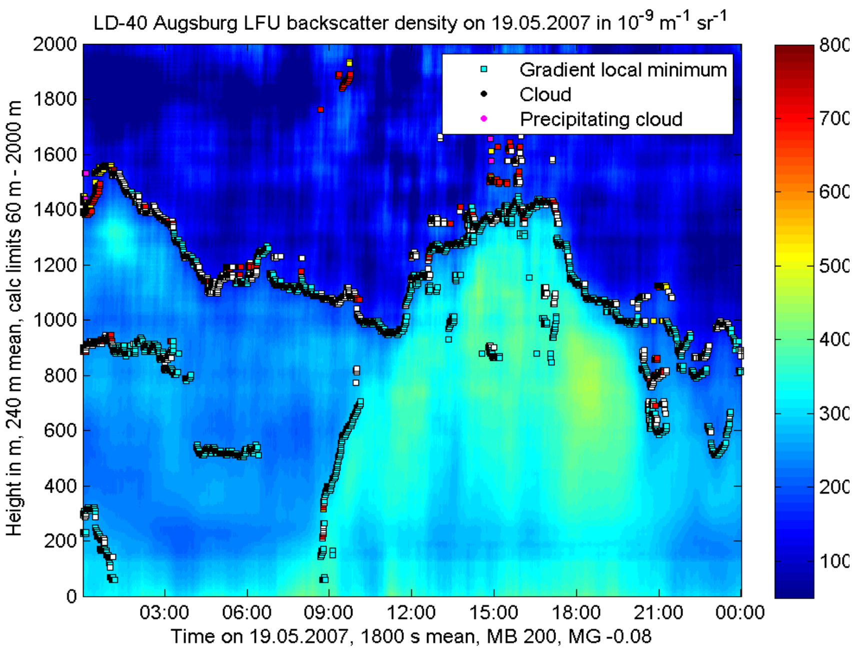

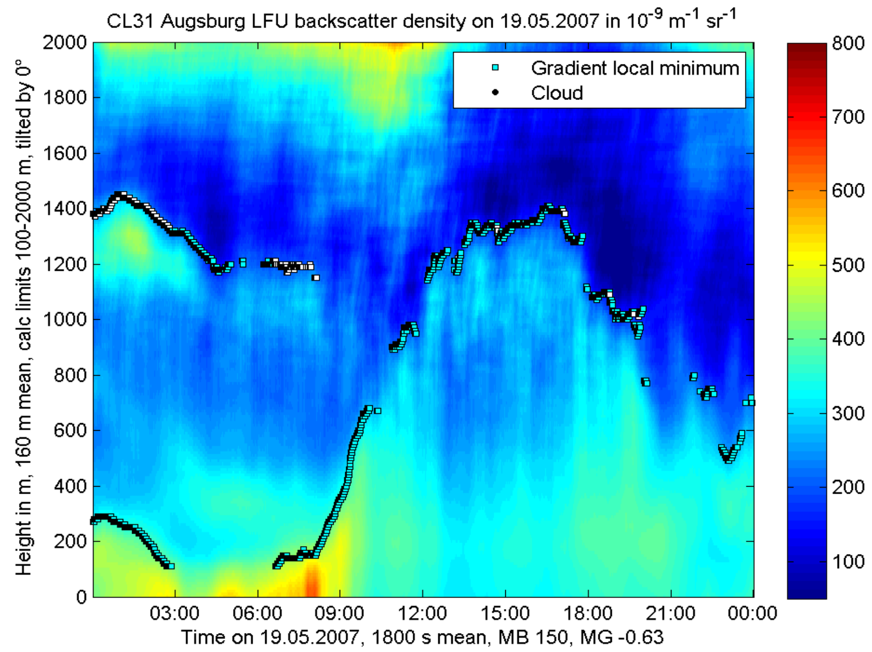

Application examples for SODAR and Ceilometer

KIT – die Kooperation von
Forschungszentrum Karlsruhe GmbH
und Universität Karlsruhe (TH)

HELMHOLTZ GEMEINSCHAFT

Forschungszentrum Karlsruhe
in der Helmholtz-Gemeinschaft

SODAR measurements in a wintry Alpine valley

29 January 2006

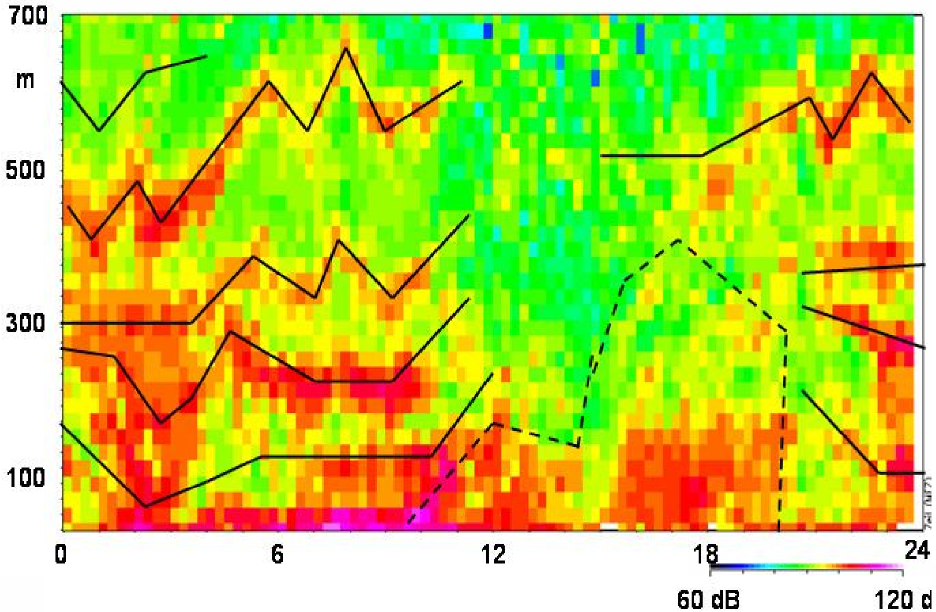

backscatter intensity

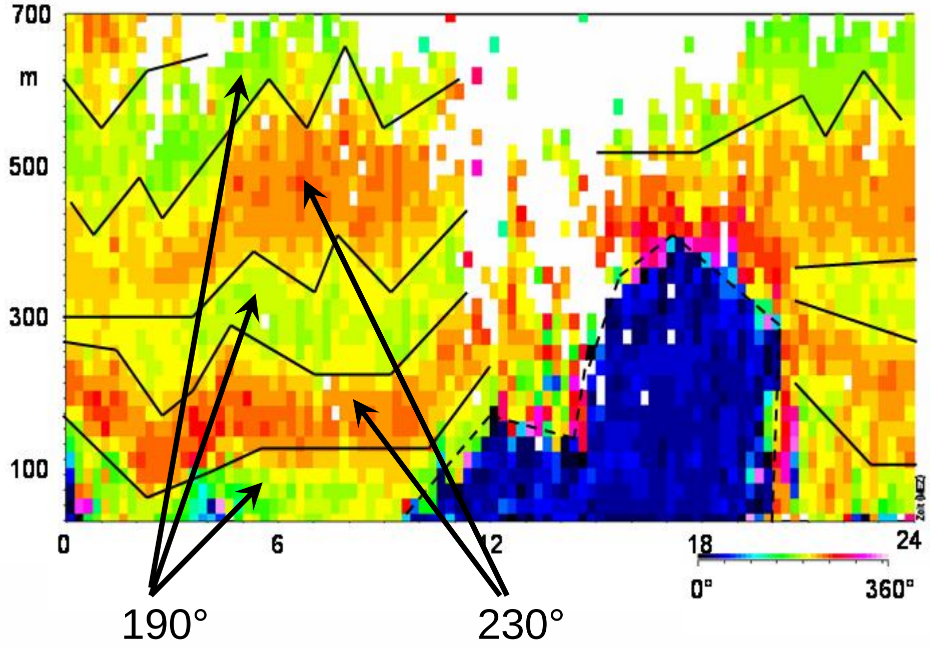

wind direction

Diurnal variation of mixing-layer height from SODAR and Ceilometer data (Budapest)

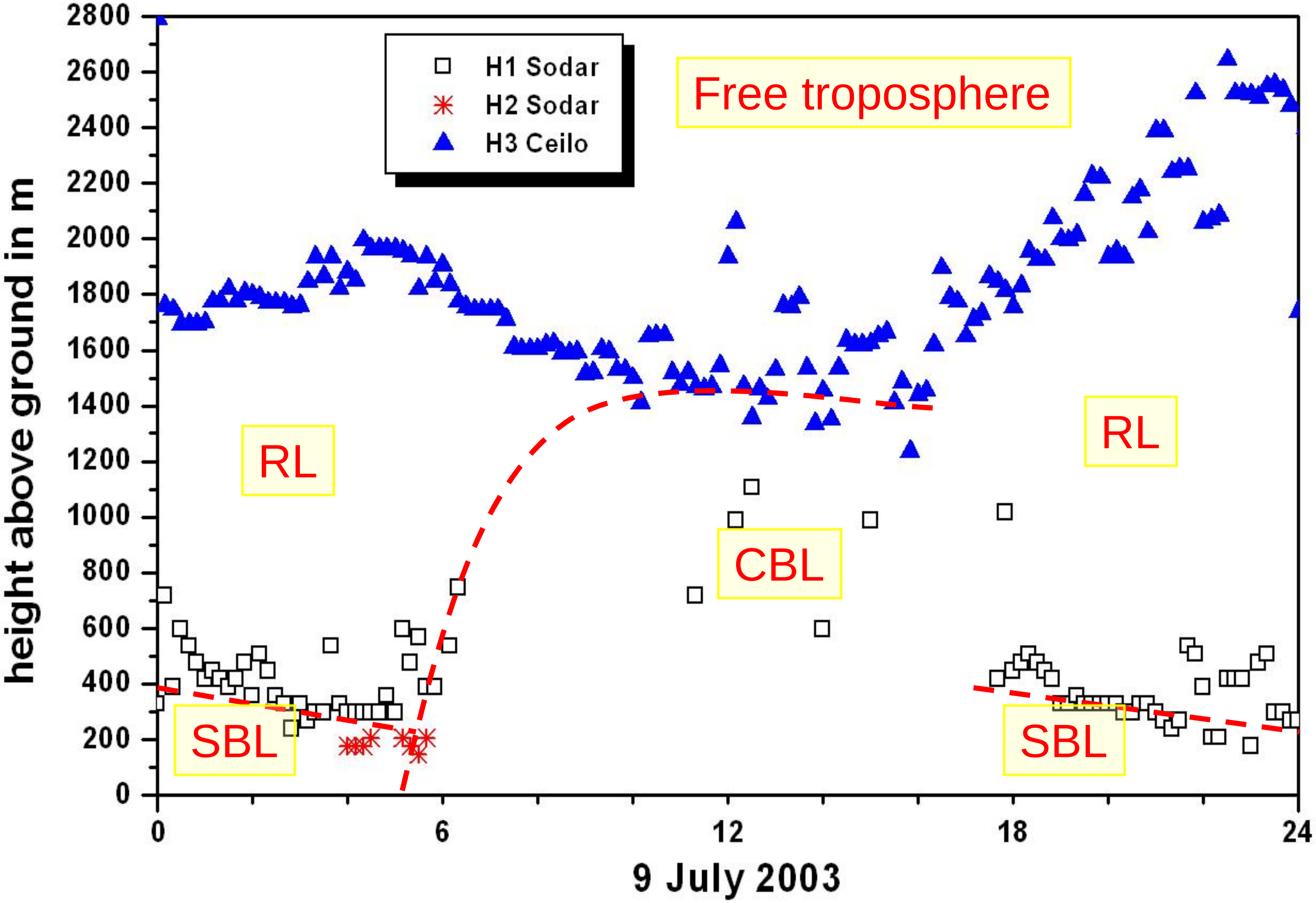

SBL:

stable boundary layer (usually at night and in winter)

CBL:

convective boundary layer (usually at daytime due to strong insolation)

RL:

residual layer (usually at nighttime)

Simultaneous operation SODAR-Ceilometer: examples for summer days

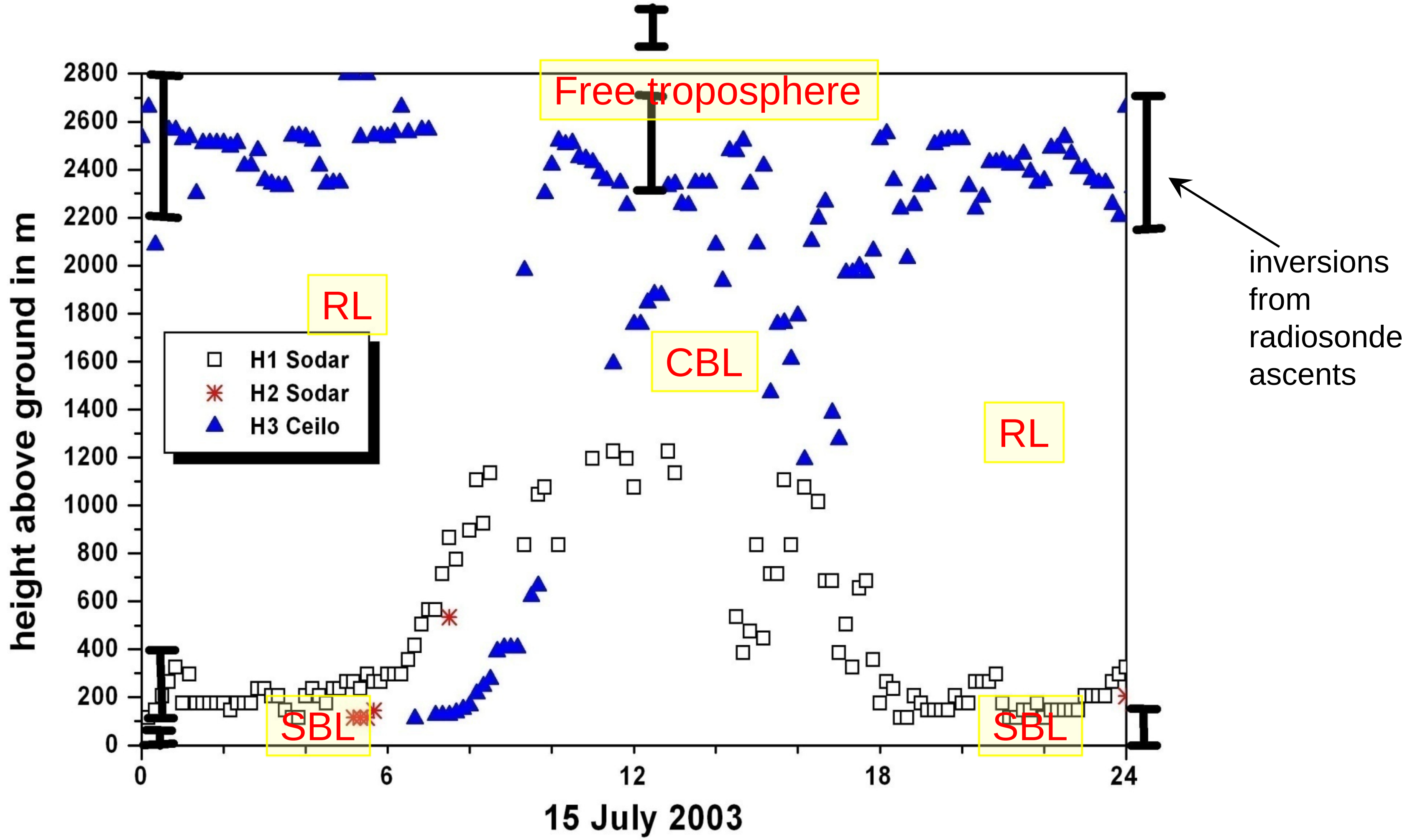

Emeis, S., K. Schäfer, 2006: Remote sensing methods to investigate boundary-layer structures relevant to air pollution in cities. Bound.-Lay Meteorol., 121, 377-385,

comparison of optical (top) and acoustic (below) backscatter intensity

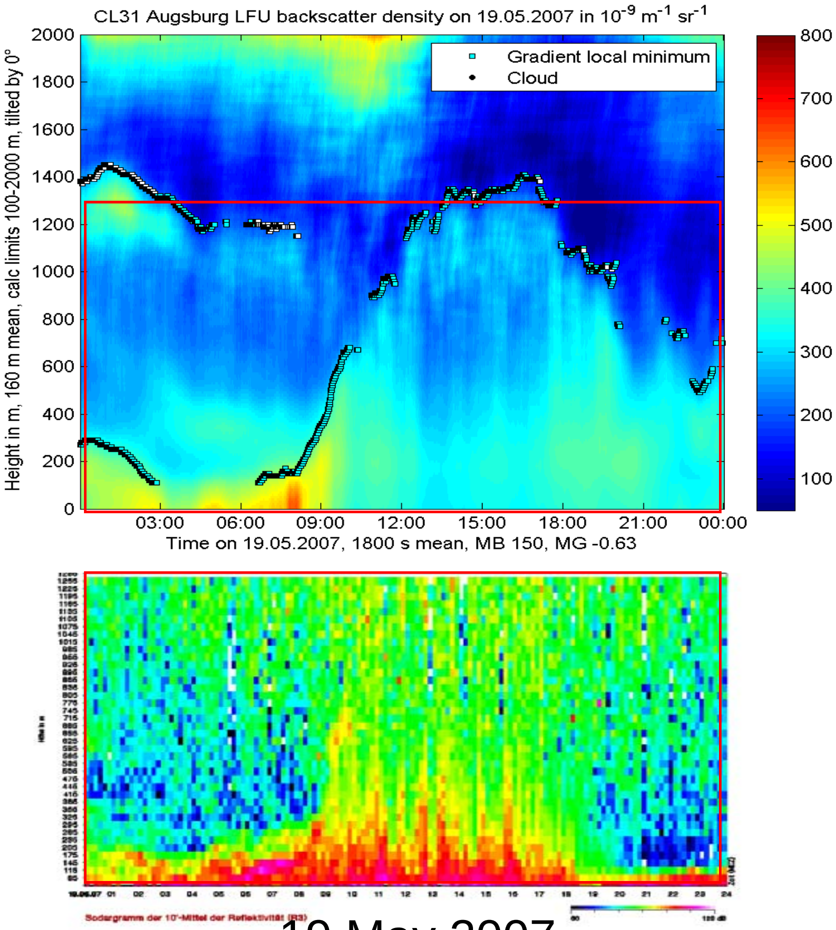

19 May 2007

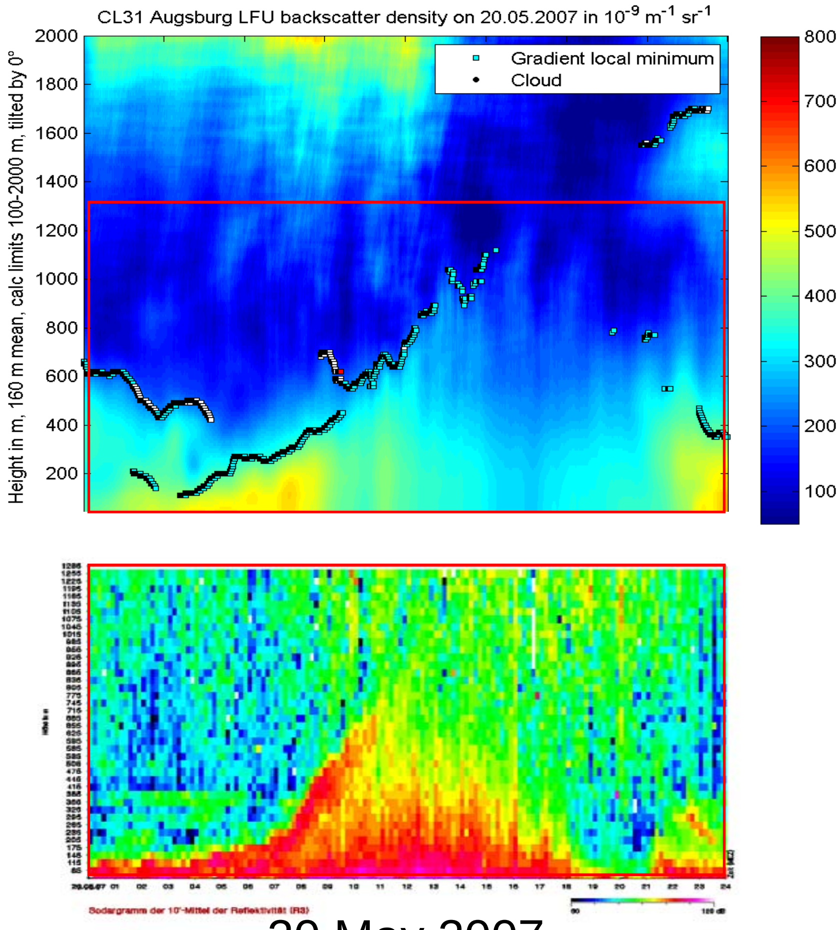

20 May 2007

comparison of MLH from Sodar and CL31 data

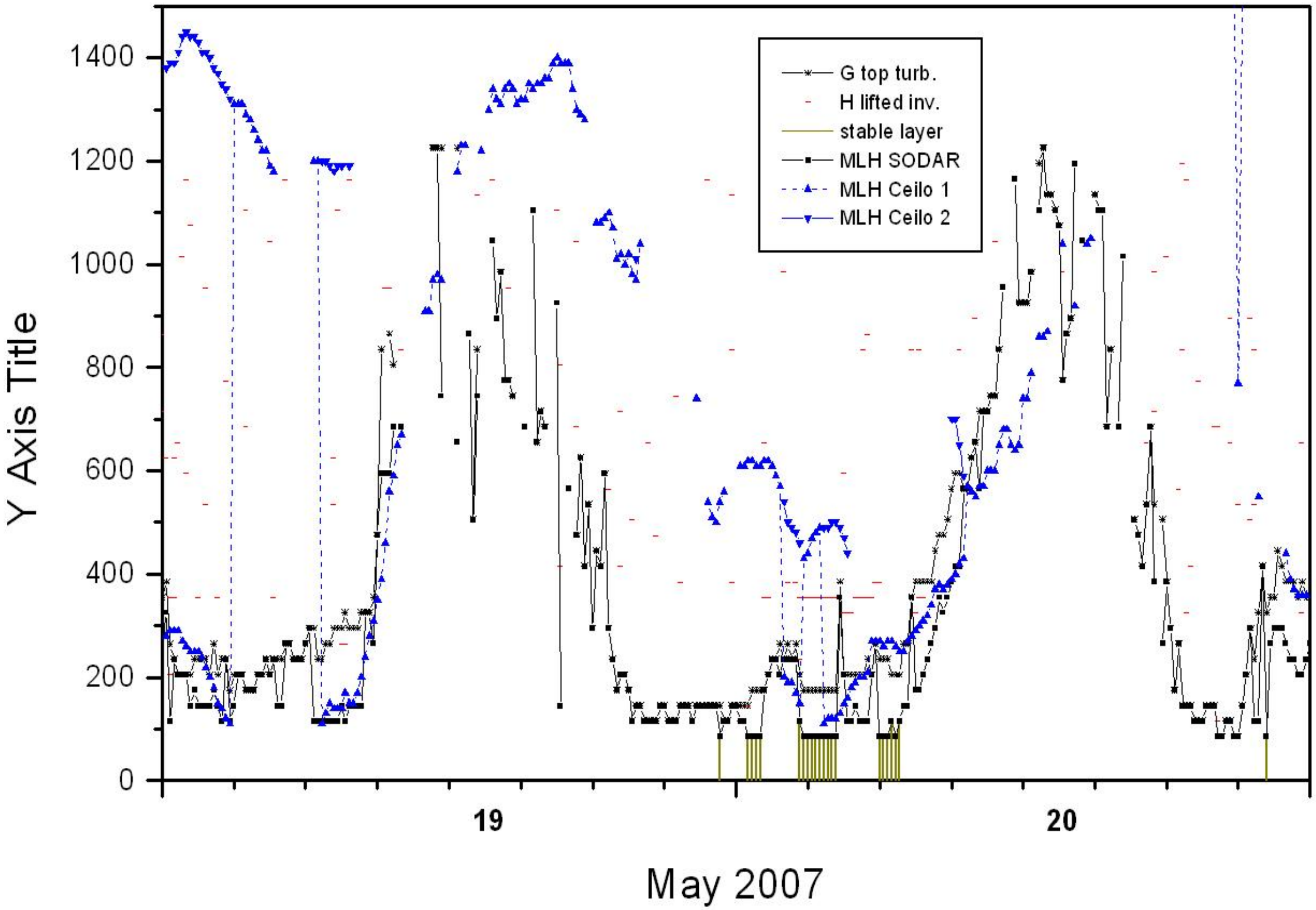

RASS

principles of operation

examples

RASS (radio-acoustic remote sensing)

measures vertical temperature profiles

Bragg-RASS: windprofiler plus acoustic component

Doppler-RASS: SODAR plus electro-magnetic component

UHF RASS (boundary layer)

VHF RASS (troposphere)

RASS: frequencies

Bragg condition:
acoustic wavelength = ½ electro-magnetic wavelength

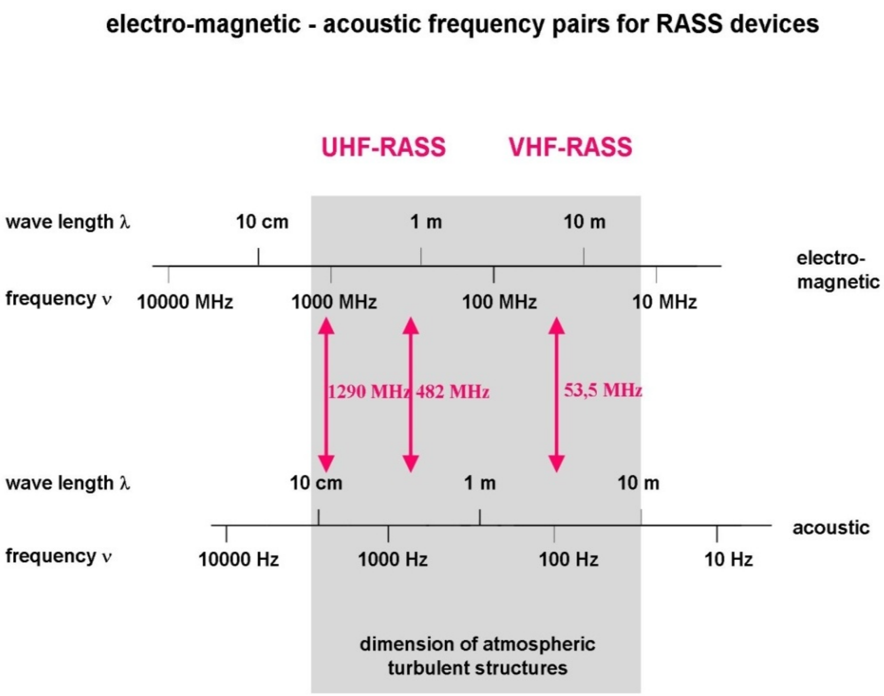

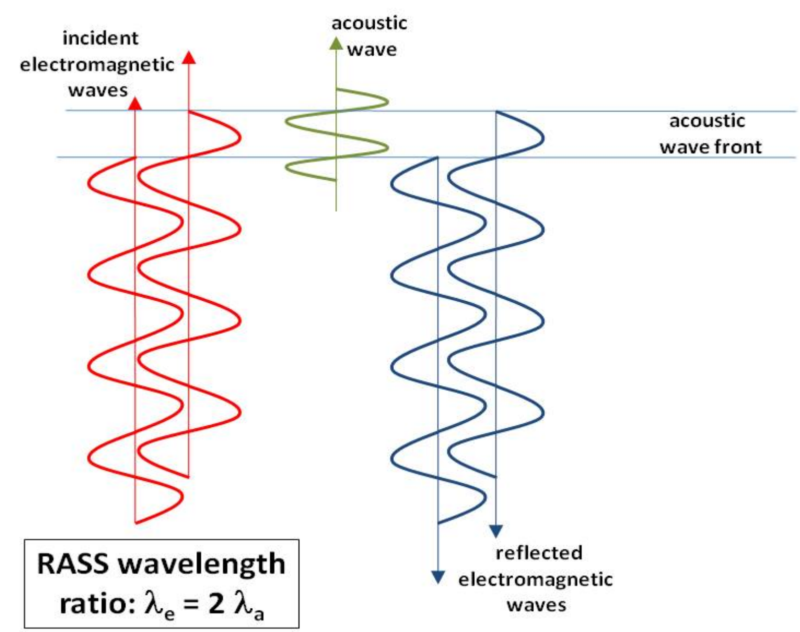

SODAR-RASS
(Doppler-RASS)

(METEK)

acoustic frequ.: 1500 – 2200 Hz
radio frequ.: 474 MHz
resolution: 20 m
lowest
range gate: ca. 40 m

vertical range: 540 m

temperature profile and dynamics

example RASS data: summer day
potential temperature (left), horizontal wind (right)

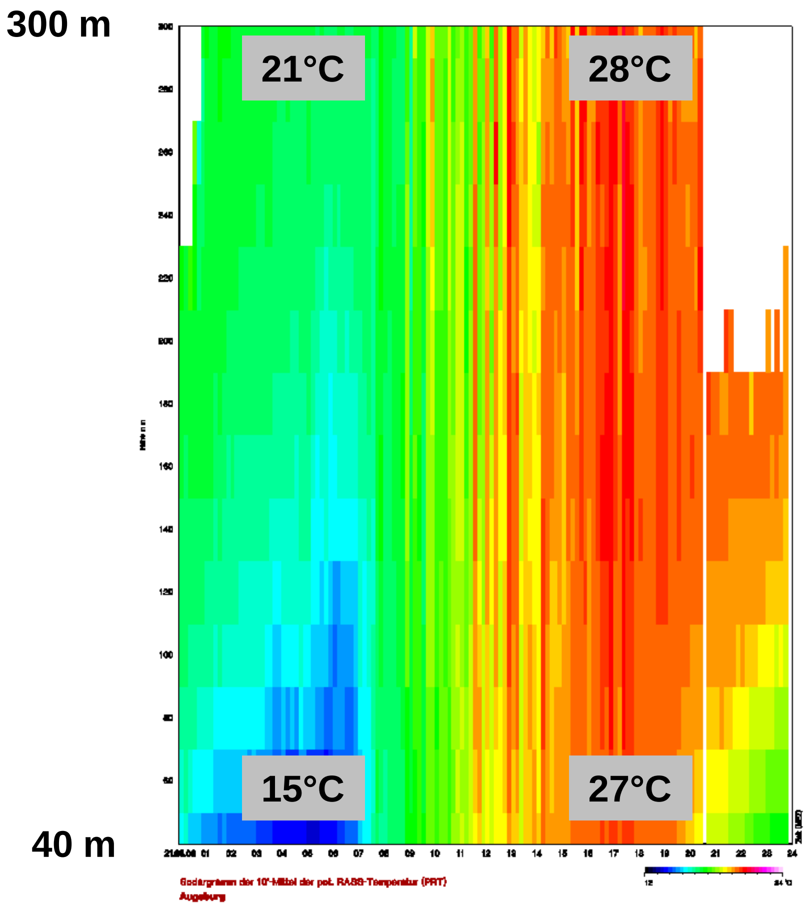

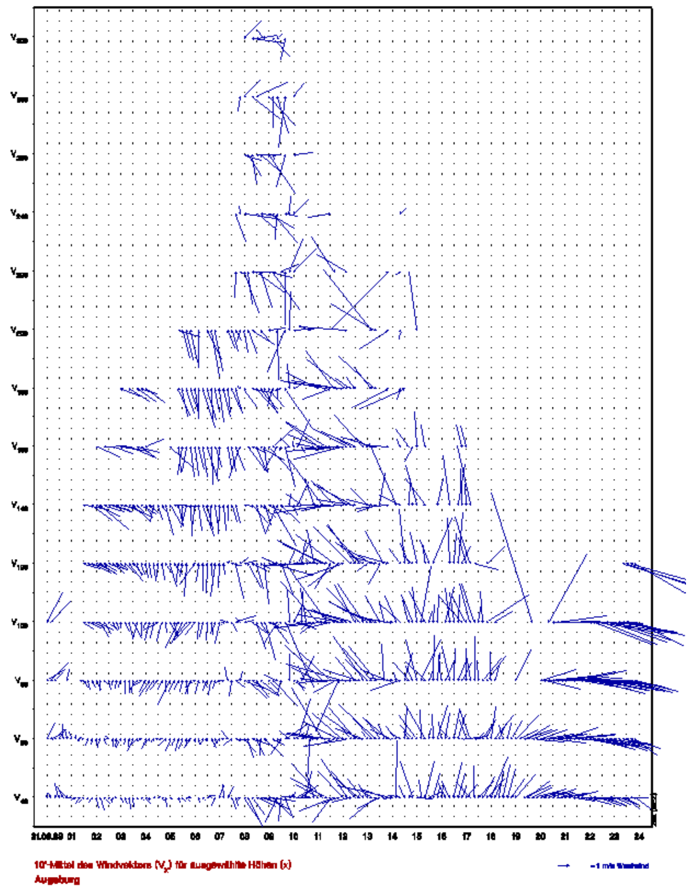

temperature profile and dynamics

example RASS data: winter day
potential temperature (left), horizontal wind (right)

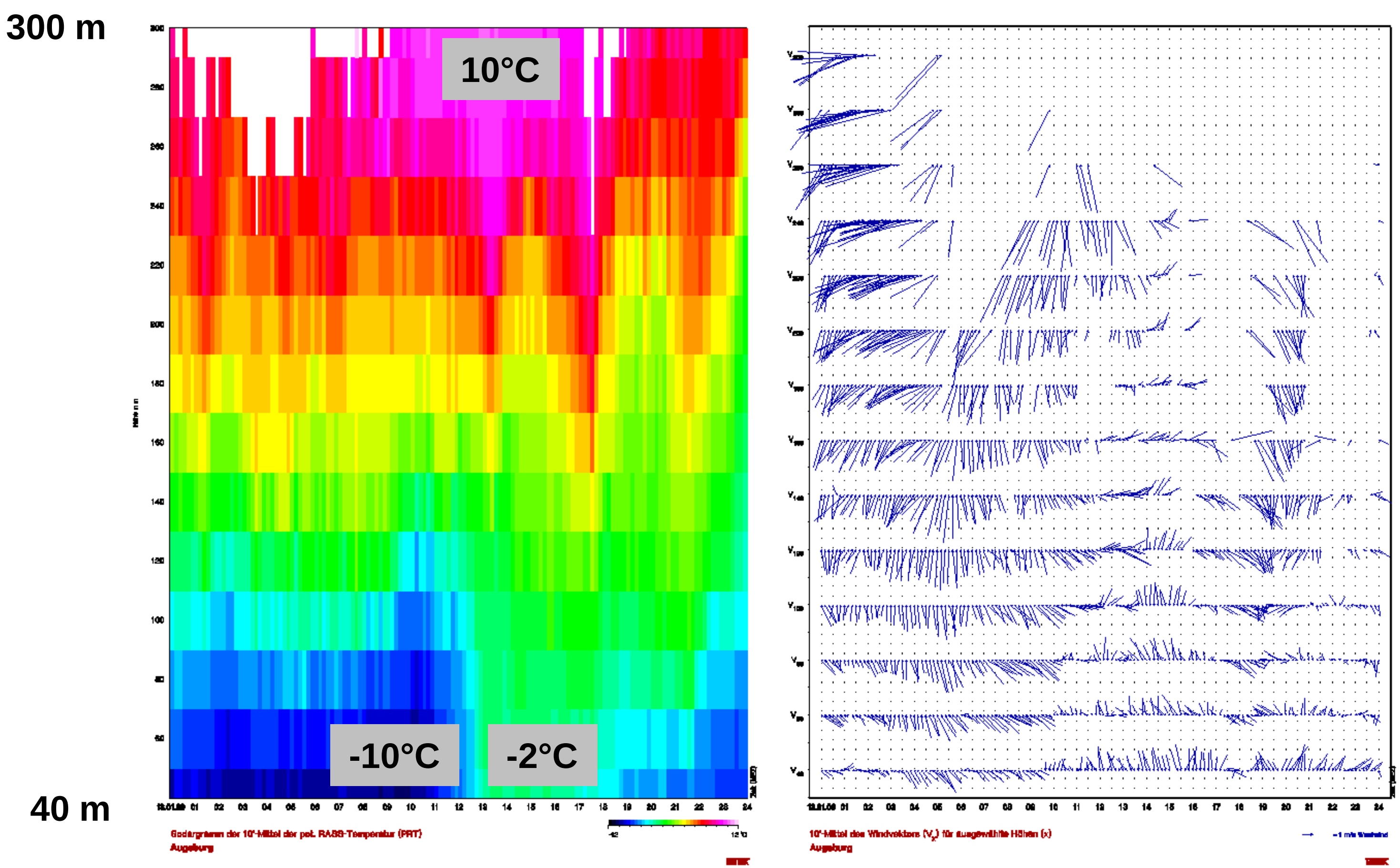

temperature profile and pollution

comparison of RASS data (potential temperature, right) with aerosol backscatter from a ceilometer (left)

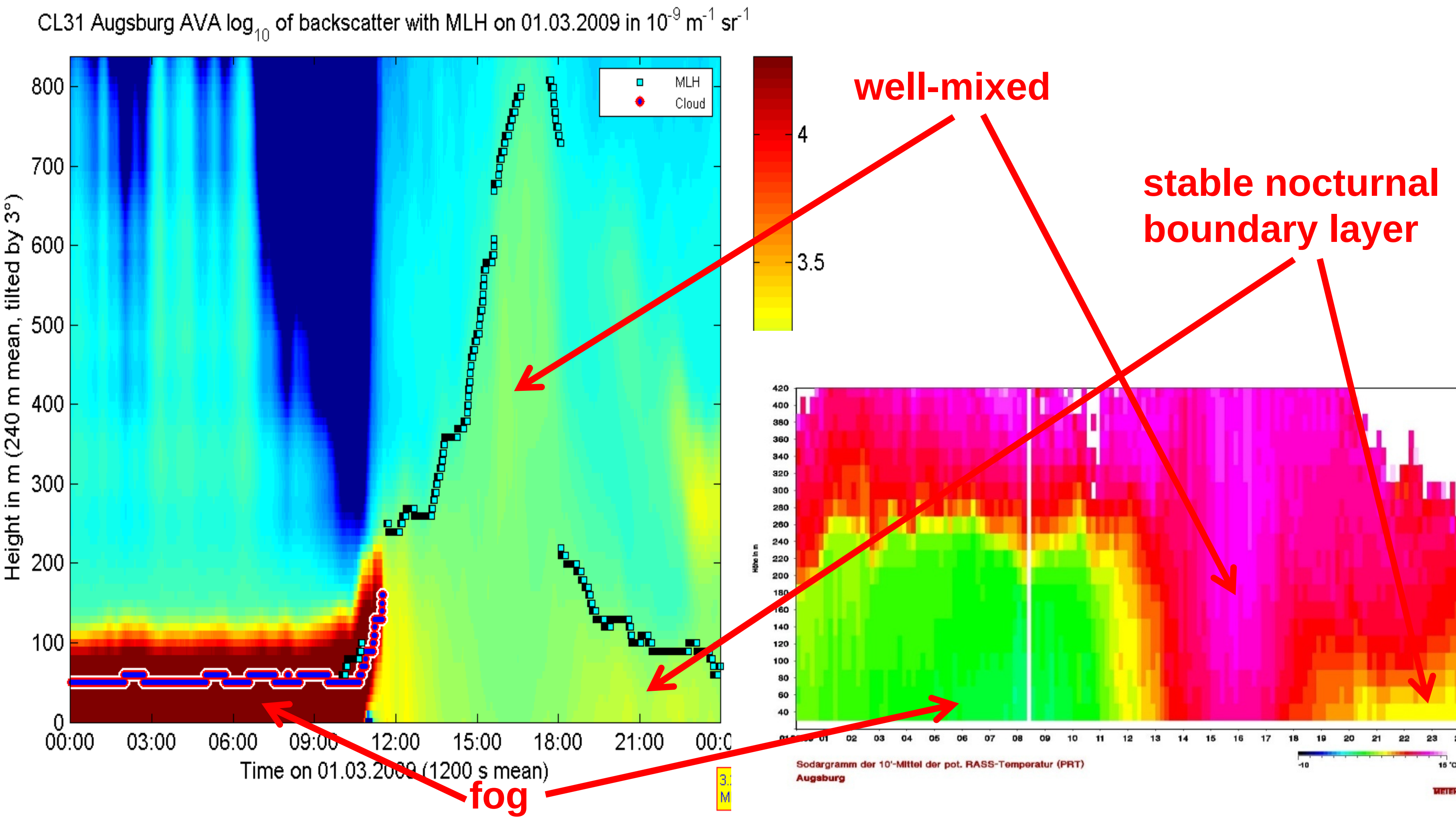

RASS data Augsburg February 2009

potential temperature (top), backscatter SODAR (middle), Ceilometer (bottom)

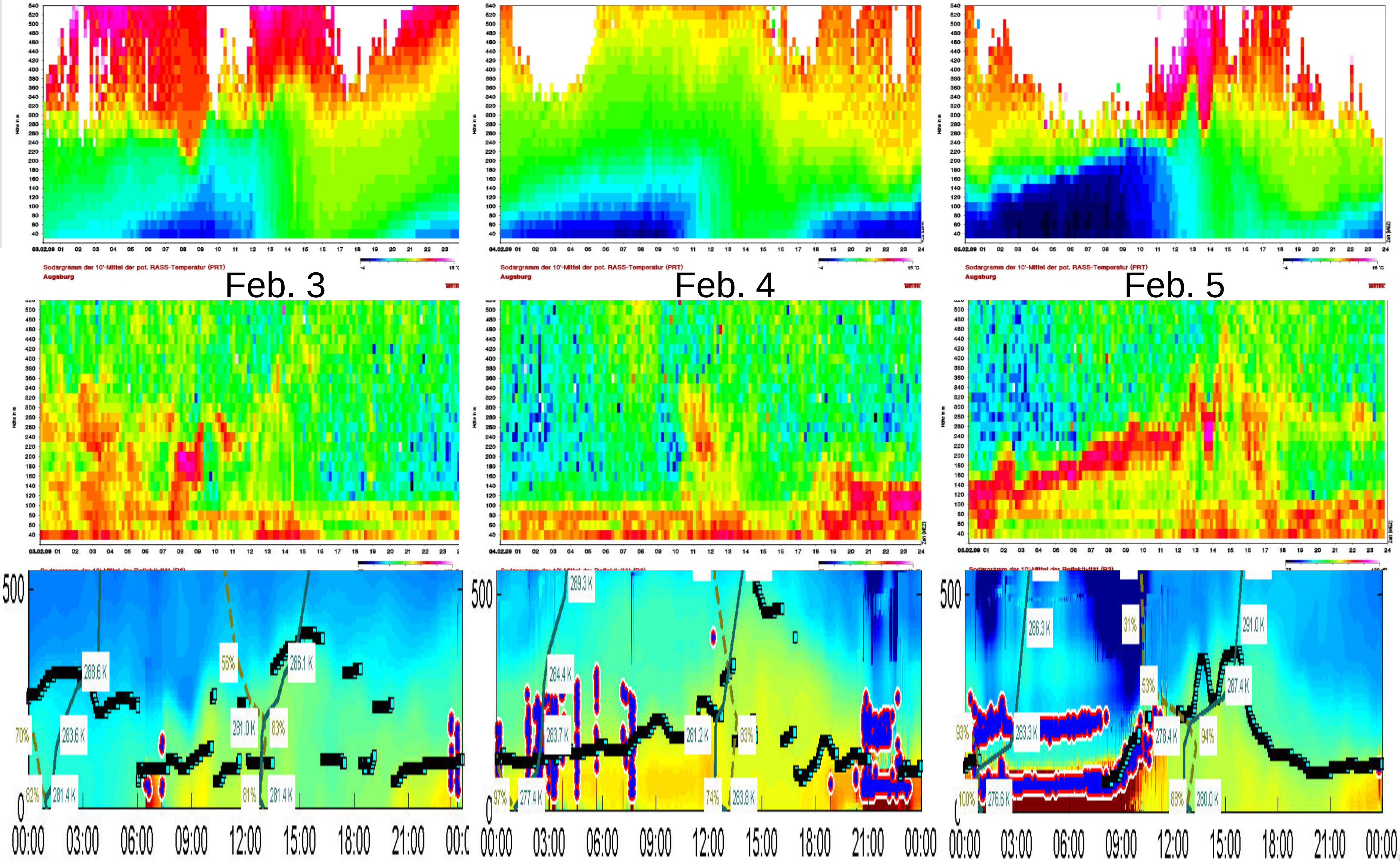

RASS data Augsburg February 2009

potential temperature (top), MLH RASS (middle), MHL SODAR/Ceilo (bottom)

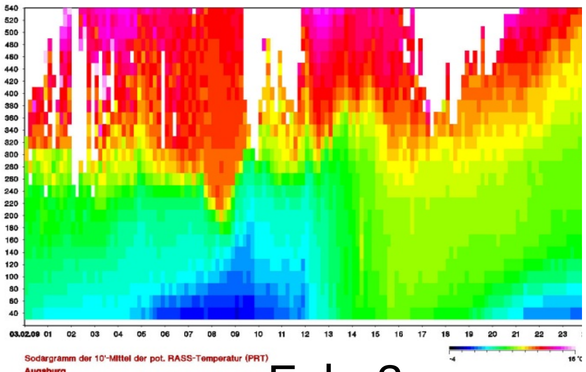

Feb. 3

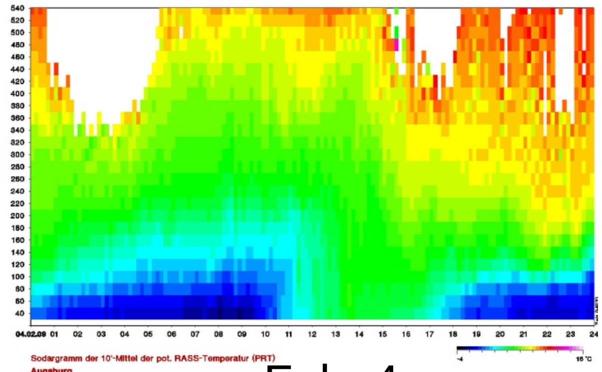

Feb. 4

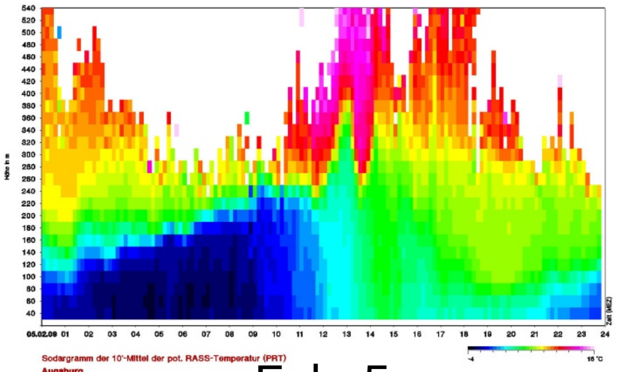

Feb. 5

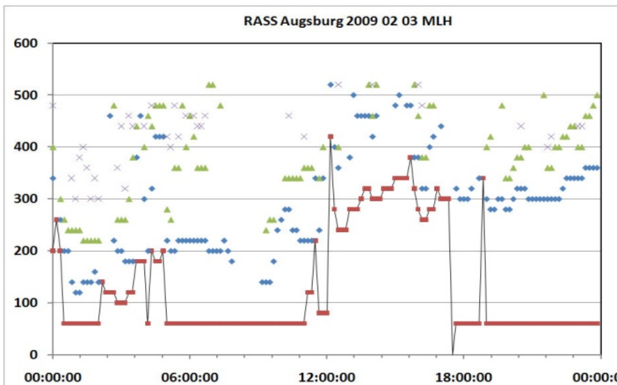

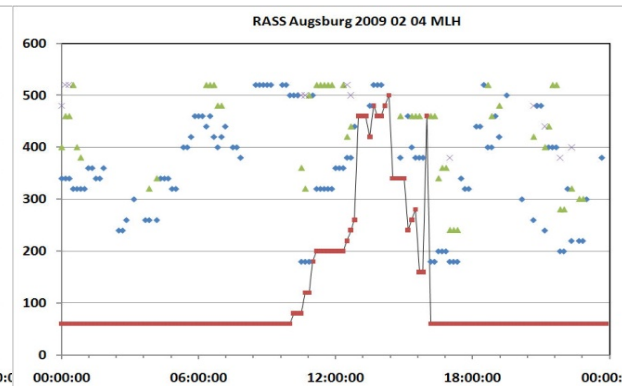

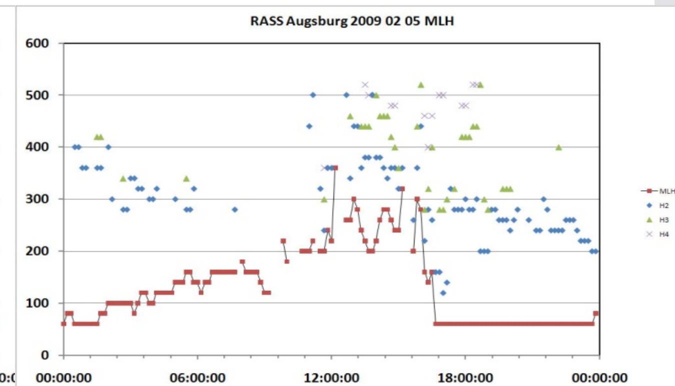

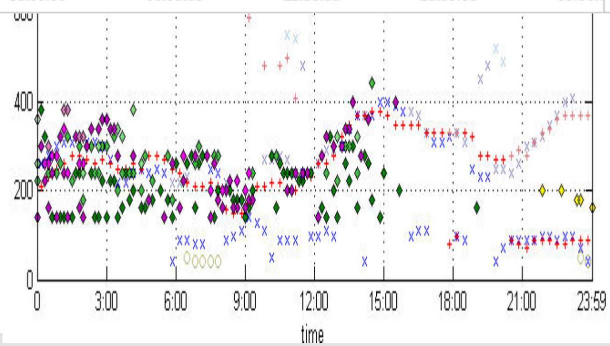

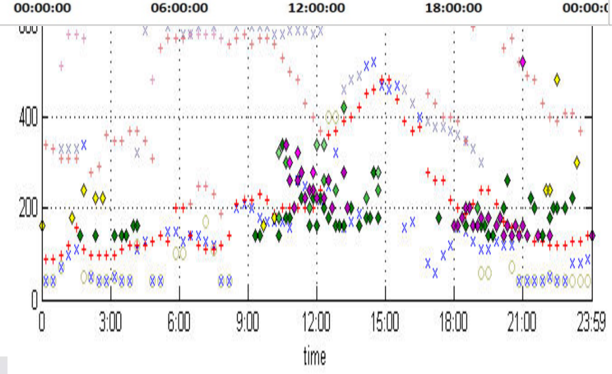

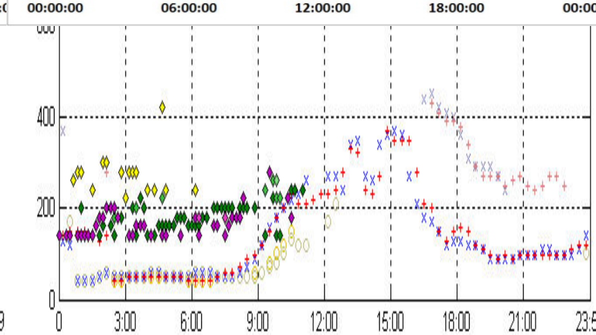

Application

Determination of regional surface emission fluxes of a substance e

Assumptions:

- **horizontal homogeneity**
- **no fluxes through the upper boundary (inversion)**
- **no sources and sinks within the volume of interest**

$$\int_{S_{surf}} \overline{e'w'} \cdot dS = \int_{V} \frac{de}{dt} dV$$

simultaneous measurement of concentration and MLH

(inverse method)

c_{CH4}

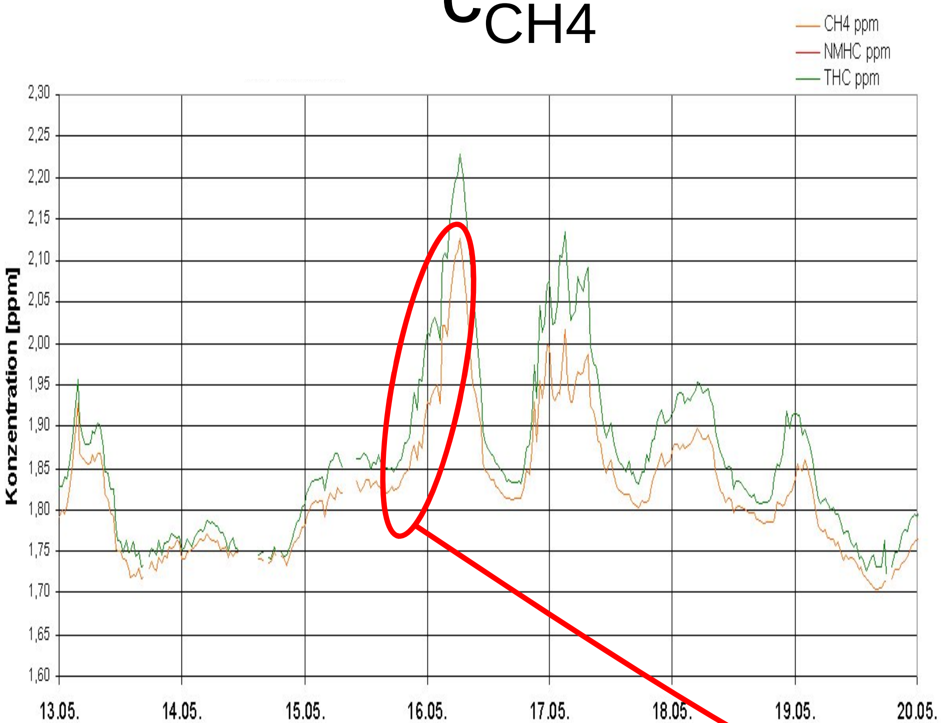

MLH

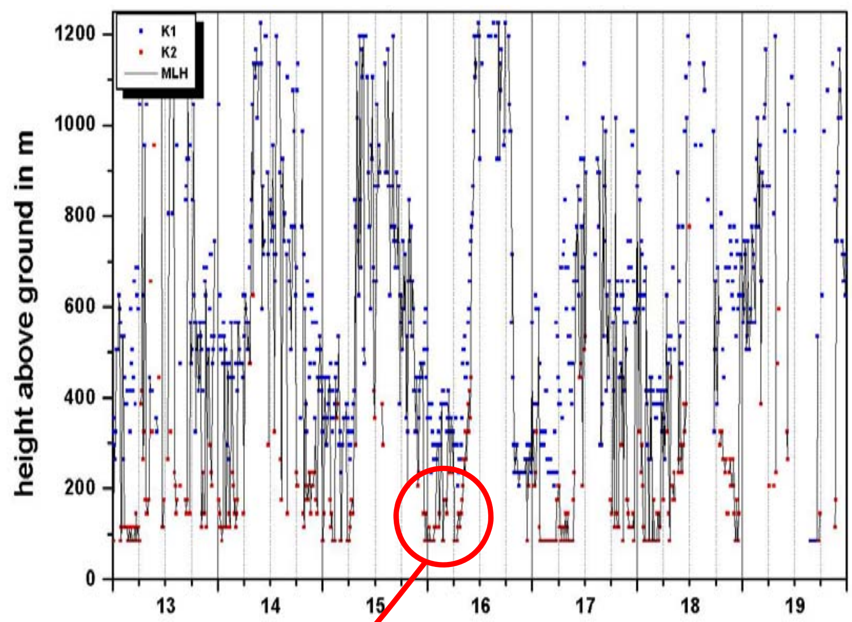

13.-19.05.2003

simultaneous measurement of concentration and MLH

(inverse method)

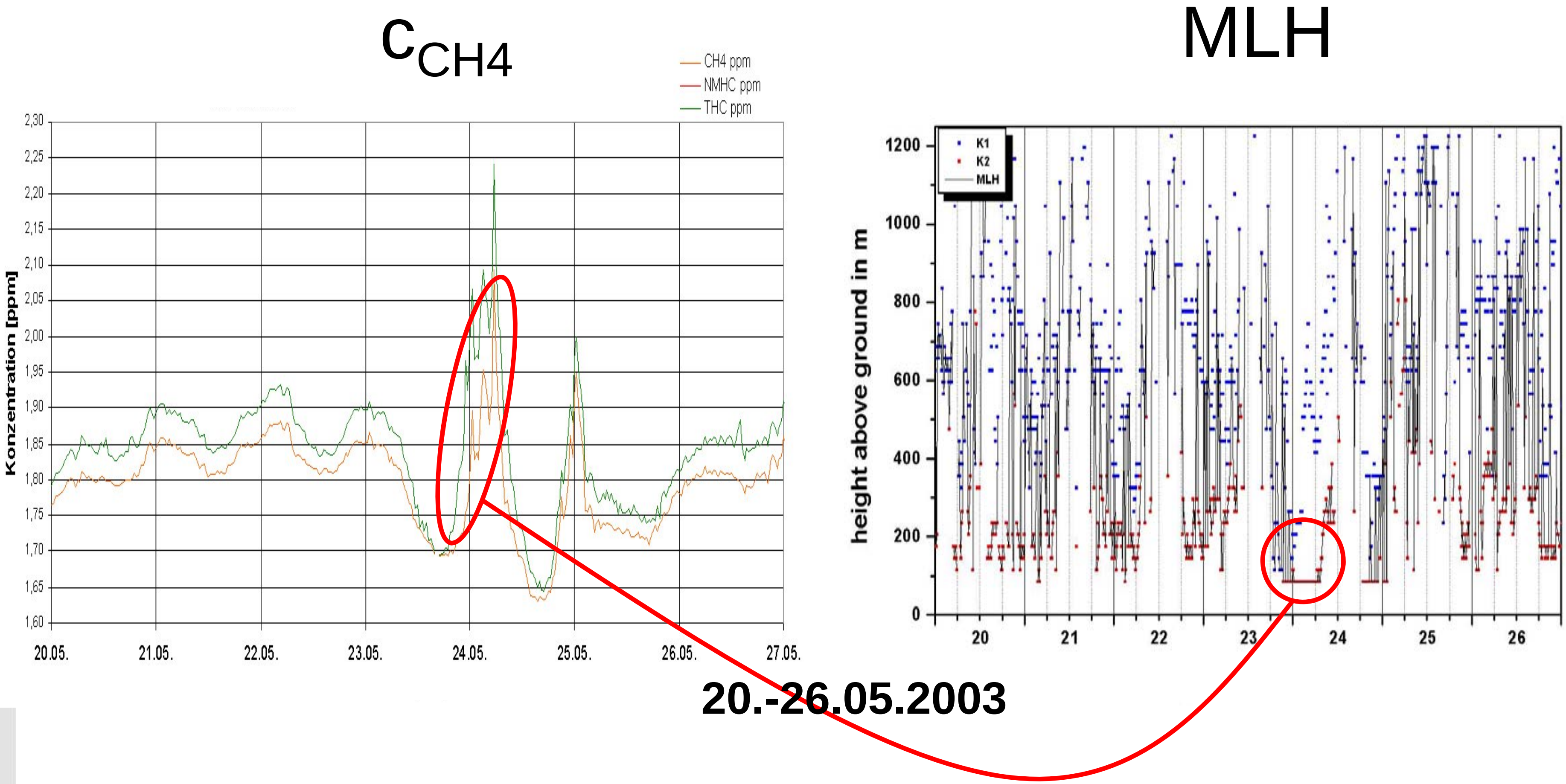

20.-26.05.2003

determination of regional $[C_{CH4}{}'w']_{surf}$ (curves) from concentration changes (x-axis) and MLH (y-axis)

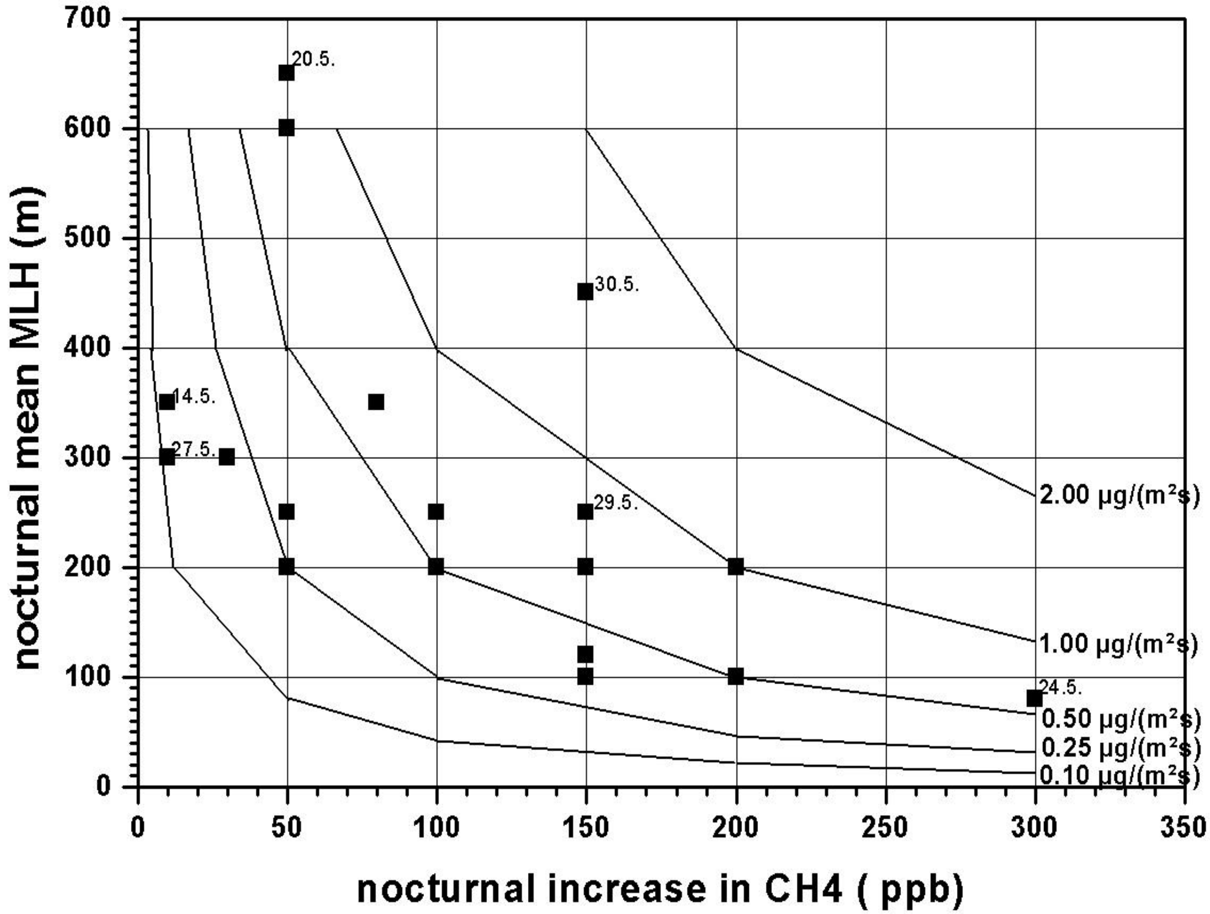

determination of regional $[C_{CH4}{'}w{'}]_{surf}$ (curves) from concentration changes and remotely sensed MLH

methane emissions:

typical values obtained here:

span:	0.10 to 2.00 µg/(m² s)
mean value:	0.50 µg/(m² s)

average values from national reporting (Kyoto protocol):

for entire Germany:	0.20 µg/(m² s)
among this from agriculture:	0.13 µg/(m² s)

Summary

Comparison of MLH retrievals with three different remote sensing techniques

SODAR
acoustic backscatter

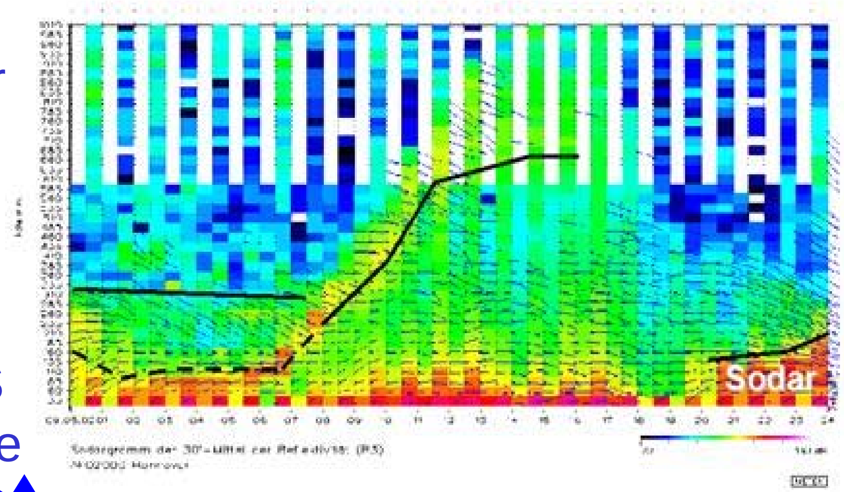

ceilometer
optical backscatter

RASS
temperature

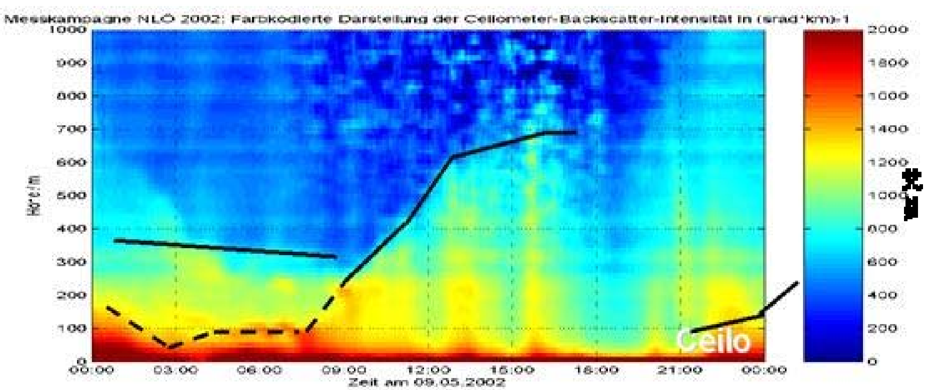

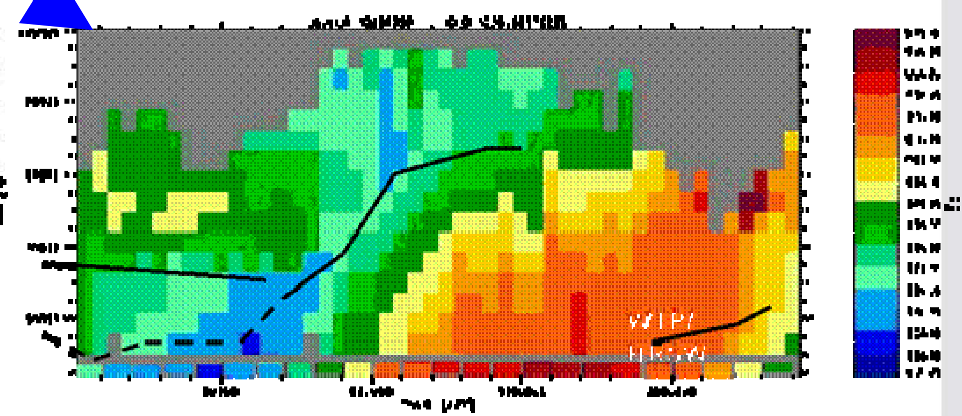

Emeis, S., Chr. Münkel, S. Vogt, W.J. Müller, K. Schäfer, 2004: Atmospheric boundary-layer structure from simultaneous SODAR, RASS, and ceilometer measurements. Atmos. Environ., 38, 273-286.

Overview on methods using ground-based remote sensing for the derivation of the mixing-layer height

method		short description
acoustic	ARE method	analysis of **a**coustic **r**eceived **e**cho intensity profiles
“	HWS method	analysis of **h**orizontal **w**ind **s**peed profiles
“	VWV method	analysis of **v**ertical **w**ind **v**ariance profiles
“	EARE method	analysis of acoustic backscatter intensity and vertical wind variance profiles (**e**nhanced **a**coustic **r**eceived **e**cho method)
optical	threshold method	detection of a given backscatter intensity threshold
“	gradient method	analysis of optical backscatter intensity profiles
“	idealised backscatter method	analysis of optical backscatter intensity profiles
“	wavelet method	analysis of optical backscatter intensity profiles
“	variance method	analysis of optical backscatter intensity profiles
acoustic / electro-magnetic		ARE method applied to sodar and wind profiler data
acoustic / optical		EARE method plus gradient method
electro-magnetic / electro-magnetic		combination of a sodar-RASS and a wind profiler RASS: analysis of the vertical temperature profile plus analysis of the electro-magnetic backscatter intensity profile
acoustic / in situ		ARE method plus in-situ surface flux measurement

RASS	analysis of the temperature profile from the measured speed of sound

Conclusions:

RASS directly delivers temperature profiles,
MLH, inversions, and stable layers can easily be detected,
wind profiles are additionally available.
Does not work properly with high wind speeds.

SODAR detects temperature fluctuations and gradients, but no absolute temperature. Inversions and stable layers can indirectly be inferred with a MLH algorithm.
Does not work properly with perfectly neutral stratification, with very high wind speeds, and during stronger precipitation events.

Ceilometer detects aerosol distribution and water droplets. It has to be assumed that the aerosol follows the thermal structure of the atmosphere. Inversions and MLH can indirectly be inferred with a MLH algorithm.
Does not work properly in extreme clear (aerosol-free) air and during precipitation events and fog.

Literature

SODAR:

Asimakopoulos, D.N., C.G. Helmis, J. Michopoulos, 2004: Evaluation of SODAR methods for the determination of the atmospheric boundary layer mixing height. - Meteor. Atmos. Phys. 85, 85–92.

Beyrich, F., 1997: Mixing height estimation from sodar data – a critical discussion. - Atmos. Environ. 31, 3941–3953.

Ceilometer:

Schäfer, K., S.M. Emeis, A. Rauch, C. Münkel, S. Vogt, 2004: Determination of mixing-layer heights from ceilometer data. In: Remote Sensing of Clouds and the Atmosphere IX. Schäfer, K., A. Comeron, M. Carleer, R.H. Picard, N. Sifakis (Eds.), Proc. SPIE, Bellingham, WA, USA, Vol. 5571, 248–259.

Sicard, M., C. Pérez, F. Rocadenbosch, J.M. Baldasano, D. García-Vizcaino, 2006: Mixed-Layer Depth Determination in the Barcelona Coastal Area From Regular Lidar Measurements: Methods, Results and Limitations. - Bound.-Lay. Meteor. 119, 135–157.

RASS:

Engelbart, D.A.M., J. Bange, 2002: Determination of boundary-layer parameters using wind profiler/RASS and sodar/RASS in the frame of the LITFASS project. Theor. Appl. Climatol. 73, 53–65.

Emeis, S., K. Schäfer, C. Münkel, 2009: Observation of the structure of the urban boundary layer with different ceilometers and validation by RASS data. Meteorol. Z., 18, 149-154. (Open access, freely avaiable from http://dx.doi.org/10.1127/0941-2948/2009/0365)

Reviews:

Emeis, S., K. Schäfer, C. Münkel, 2008: Surface-based remote sensing of the mixing-layer height – a review. - Meteorol. Z., 17, 621-630. (Open access, freely available from http://dx.doi.org/10.1127/0941-2948/2008/0312)

Emeis, S., M. Harris, R.M. Banta, 2007: Boundary-layer anemometry by optical remote sensing for wind energy applications. - Meteorol. Z., 16, 337-347.

Thank you very much for your attention